

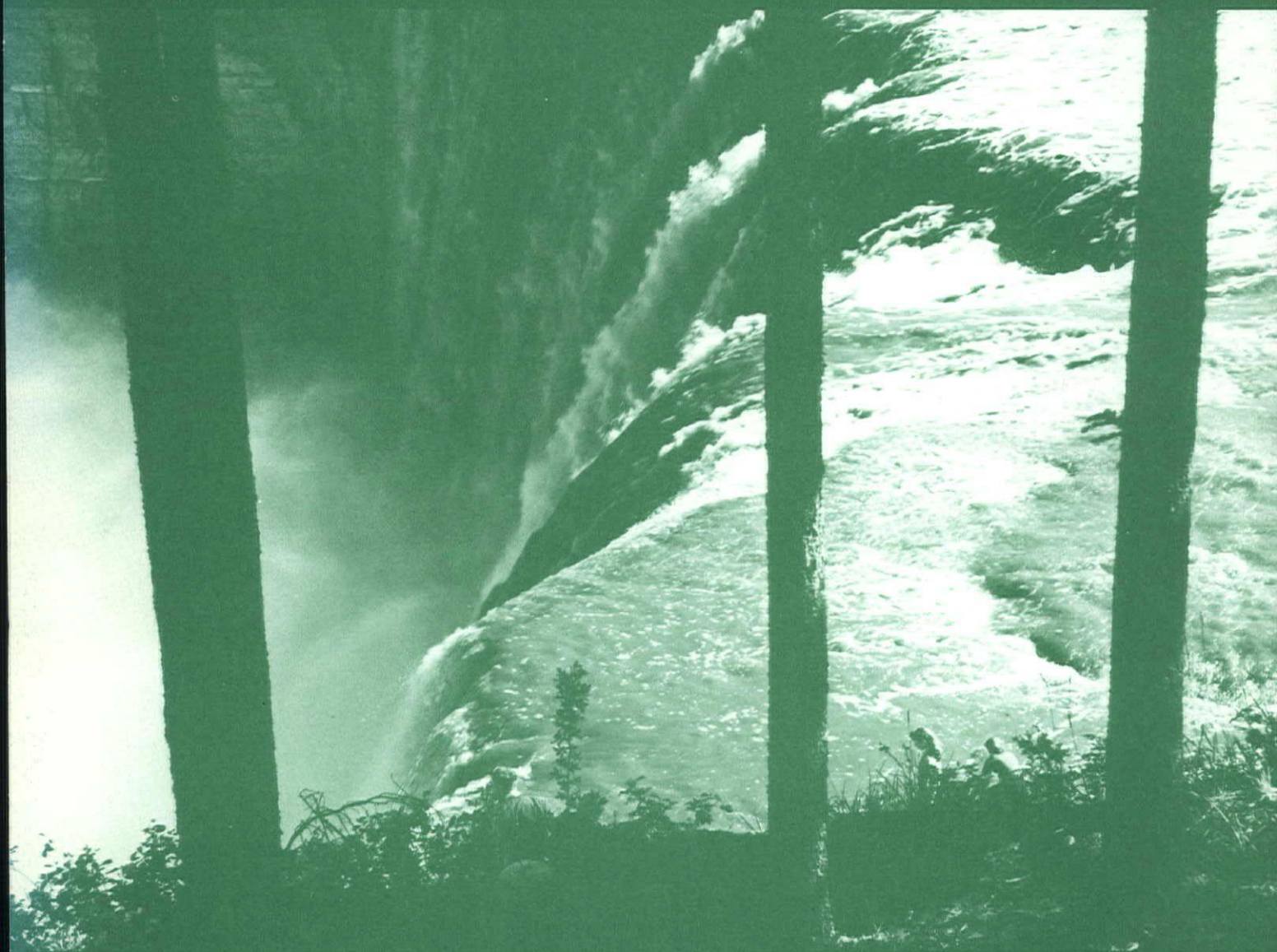


Environment
Canada

Environnement
Canada

Further Climatological Studies of Baffin Island, Northwest Territories

R.G. Barry



TECHNICAL BULLETIN NO. 65

*INLAND WATERS DIRECTORATE,
WATER RESOURCES BRANCH,
OTTAWA, CANADA, 1974*



Environment
Canada

Environnement
Canada

Further Climatological Studies of Baffin Island, Northwest Territories

R.G. Barry

TECHNICAL BULLETIN NO. 65

***INLAND WATERS DIRECTORATE,
WATER RESOURCES BRANCH,
OTTAWA, CANADA, 1974***

©
Information Canada
Ottawa, 1973

Cat. No.: En36-503/65

CONTRACT #02KXKL327-3-8060
THORN PRESS LIMITED

Contents

	Page
1. THE FLUX DIVERGENCE OF WATER VAPOUR OVER THE EASTERN CANADIAN ARCTIC	1
2. A PRESSURE PATTERN CLASSIFICATION FOR BAFFIN ISLAND	31
3. THE SYNOPTIC CLIMATOLOGY OF PRECIPITATION AND MOISTURE FLUX	39

Foreword

This report concludes the programme of climatological investigations of Baffin Island begun in September 1966 as a part of the Baffin-Island Project (G-67-12) of the Department of Energy, Mines and Resources and continued under Project 16 of the land-based ice studies. This final report contains the results of work undertaken by Dr. Barry between October 1968 and July 1971 at the Institute of Arctic and Alpine Research, University of Colorado, Boulder.

Several individuals have contributed to this investigation. Particular thanks are due to Mr. K. Shimizu and his assistants in the Division of Quaternary Research and Geomorphology, Geological Survey of Canada, for writing the necessary programmes and organizing the data processing. Miss M. Strome assisted with various stages of the data preparation. Records for Egedesminde were kindly made available by the Danske Meteorologiske Institut, Copenhagen, and for Alert, Eureka, Isachsen and Mould Bay by the Directorate of Physical Research (Geophysics), Defence Research Board of Canada.

1. The Flux Divergence of Water Vapour over the Eastern Canadian Arctic

Contents

	Page
INTRODUCTION	5
METHODS	5
RESULTS	6
Flux divergence	6
Comparison of flux divergence of water vapour and moisture budget data	7
CONCLUSIONS	9
REFERENCES	11
APPENDIX 1. Stations for which upper air data were used in the analysis	29

Illustrations

Figure 1. Flux divergence, January 1961	15
Figure 2. Flux divergence, January 1962	15
Figure 3. Flux divergence, January 1963	16
Figure 4. Flux divergence, January 1964	16
Figure 5. Flux divergence, January 1965	17
Figure 6. Flux divergence, April 1961	17
Figure 7. Flux divergence, April 1962	18
Figure 8. Flux divergence, April 1963	18
Figure 9. Flux divergence, April 1964	19
Figure 10. Flux divergence, April 1965	19
Figure 11. Flux divergence, July 1961	20
Figure 12. Flux divergence, July 1962	20
Figure 13. Flux divergence, July 1963	20
Figure 14. Flux divergence, July 1964	20
Figure 15. Flux divergence, July 1965	21
Figure 16. Flux divergence, October 1961	21
Figure 17. Flux divergence, October 1962	22
Figure 18. Flux divergence, October 1963	22
Figure 19. Flux divergence, October 1964	23
Figure 20. Flux divergence, October 1965	23
Figure 21. Rawinsonde stations and flux-divergence triangles	24
Figure 22. Mean flux divergence, January, 1961-65	25

Illustrations (cont.)

	Page
Figure 23. Mean flux divergence, April, 1961-65	25
Figure 24. Mean flux divergence, October, 1961-65	26
Figure 25. Mean flux divergence, mean winter season, 1961-65	26
Figure 26. Mean flux divergence, July 1961-65	26
Figure 27. Profiles of flux divergence for selected triangles: Frobisher-Clyde-Hall Beach; Egedesminde-Clyde-Frobisher; Egedesminde-Thule-Clyde. January 1961-65 . .	27
Figure 28. Profiles of flux divergence for selected triangles: Frobisher-Clyde-Hall Beach; Egedesminde-Clyde-Frobisher; Egedesminde-Thule-Clyde. April 1961-65	27
Figure 29. Profiles of flux divergence for selected triangles: Frobisher-Clyde-Hall Beach; Egedesminde-Clyde-Frobisher; Egedesminde-Thule-Clyde. July 1961-65	28
Figure 30. Profiles of flux divergence for selected triangles: Frobisher-Clyde-Hall Beach; Egedesminde-Clyde-Frobisher; Egedesminde-Thule-Clyde. October 1961-65 . .	28

Tables

1. Monthly flux divergence of water vapour. Triangle: Frobisher-Clyde-Hall Beach	8
2. Monthly flux divergence of water vapour. Triangle: Egedesminde-Clyde-Frobisher . . .	9
3. Monthly flux divergence of water vapour. Triangle: Egedesminde-Thule-Clyde	10
4. Monthly flux divergence of water vapour. Triangle: Frobisher-Clyde-Hall Beach	10
5. Monthly flux divergence of water vapour. Triangle: Egedesminde-Clyde-Frobisher . . .	10
6. Monthly flux divergence of water vapour. Triangle: Egedesminde-Thule-Clyde	11
7. Comparison of grid and triangle estimates of vapour-flux divergence	11
8. Comparison of moisture budget and flux convergence estimates.	11

The Flux Divergence of Water Vapour over the Eastern Canadian Arctic

INTRODUCTION

The objectives of this study are to provide information on the moisture flux divergence and sources of precipitation over the eastern Canadian Arctic. Apart from the work of Boyes (1963) on the meridional advection of moisture across latitudes 65°, 70° and 80°N for January and July 1958, and the global scale study for the IGY year by Peixoto (1970), there are no data on the horizontal flux divergence of water vapour over the Arctic. Rasmusson's analysis (1968) of seasonal and annual flux divergence over North America extends only to Baffin Island.

This report represents a continuation of the work by Barry and Fogarasi (1968) on the horizontal vapour transport over Baffin Island. A related analysis of summer conditions over the Queen Elizabeth Islands has been prepared separately (Barry, 1972).

The specific topics investigated are:

1. Analysis of the vapour flux divergence over Baffin Island and adjacent areas for January, April, July and October, 1961-65.
2. Comparison of the aerological results with generalized estimates of precipitation minus evaporation.

METHODS

At any level, flux divergence of water vapour is given by

$$\nabla \cdot (\vec{V}q) = \frac{\delta(uq)}{\delta x} + \frac{\delta(vq)}{\delta y}$$

where q = vapour content

u = zonal wind (positive eastward)

v = meridional wind (positive northward)

This can be evaluated by finite difference methods over a quasi-Cartesian grid from

$$\nabla \cdot (\vec{V}q) = \frac{(uq)_2 - (uq)_1}{\delta \lambda} + \frac{(vq)_2 - (vq)_1}{\delta \phi} - \frac{vq \tan \phi}{R}$$

where $\delta \lambda$ = unit grid length of longitude

$\delta \phi$ = unit grid length of latitude

R = radius of the earth

The third term representing convergence of the meridians was allowed for in the present study by using a quasi-Cartesian grid with a variable unit of longitudinal distance ($\delta x = R \cos \phi \delta \lambda$) rather than using a fixed δx and calculating the correction term. Thus, for the grid λ, ϕ , for λ from $i = 1$ (at λ_0), m ; and for ϕ from $j = 1$ (at ϕ_0), n , we have

$$\nabla \cdot (\vec{V}q) = \frac{1}{R \cos \phi_j} \left[\frac{(uq)_{i+1,j} - (uq)_{i-1,j}}{2\delta \lambda} + \frac{(vq)_{i,j+1} \cos \phi_{j+1} - (vq)_{i,j-1} \cos \phi_{j-1}}{2\delta \phi} \right]$$

This formulation was devised and programmed for the CDC 6400 by Mr. L.D. Williams of the Institute of Arctic and Alpine Research, Boulder, Colorado. First-order boundary conditions were used, so that

$$\delta(uq)_n = uq_{n+1} - uq_{n-1} = 2(uq_n - uq_{n-1})$$

$$\text{and } \delta(vq)_n = 2(vq_n - vq_{n-1})$$

Values of vertically integrated zonal and meridional flux at 2.5° latitude and 5° longitude intervals were entered as computer input.

$$\text{Maps of } \frac{1}{g} \int_{P_s}^{P_0} \overline{uq} dp$$

$$\text{and } \frac{1}{g} \int_{P_s}^{P_0} \overline{vq} dp$$

based on twice-daily ascents, with interpolation for most of the missing data, have been prepared for January, April, July and October for each of the years 1961-65 over the areas 60°-75°N, 50°-90°W, (60°-82.5°N, 50°-110°W for July) using data previously computed for the stations listed in Appendix 1 (Barry and Fogarasi, 1968). In addition, monthly averages of

$$\frac{1}{g} \int_{P_s}^{P_0} \overline{uq} dp \quad \text{and} \quad \frac{1}{g} \int_{P_s}^{P_0} \overline{vq} dp$$

tabulated by Bock, Frazier and Welsh (1966) for 1961 and 1962 based on twice-daily records (without adjustment for missing observations) were used for stations in adjacent areas of Canada. Maps for these two years are therefore likely to be more accurate along the southern and western margins of the area. The computed fluxes were integrated between the surface (mean station pressure for each month P_s) and a level where the flux was assumed to become zero (P_0). This was taken as 280 mbar in July-August, and 320 mbar in June and September. A linear decrease was assumed from 500 mbar to this level. The program gives flux divergence values in $\text{g cm}^{-2} \text{ month}^{-1}$ at the grid points and also prepares isoline maps (Figs 1-2) on a Lambert equal-area projection. The map values are not scaled and a note as to the analysed contour interval and contour range is given on each map.

For comparison with the previous results an objective technique of determining vapour flux divergence is used for selected triangles. The basic idea is described by Bellamy (1949) with reference to wind data and it has been extended to the field of vapour flux by Hutchings (1957). The assumption is made that the flux varies linearly between the stations at the apices of the triangle. A modified approach, suggested by A.G. Matthewman* of Meteorological Office, Bracknell, Great Britain, is employed here. The flux divergence is calculated with reference to linear terms of the three fields u , v and q , with the definitions

$$u = a_0 + a_1 x + a_2 y$$

$$v = b_0 + b_1 x + b_2 y$$

$$q = c_0 + c_1 x + c_2 y$$

With sufficient accuracy, second-order terms may be neglected so that

$$\nabla \cdot (\vec{V}q) = a_0 c_1 + a_1 c_0 + b_2 c_0 + b_0 c_2$$

With the origin at the centroid of a triangle of aerological stations ($x_1 y_1; x_2 y_2; x_3 y_3$), it follows that

$$a_0 = \frac{1}{3} (u_1 + u_2 + u_3)$$

$$a_1 = \frac{\{(u_2 - u_1)(y_3 - y_1) - (u_3 - u_1)(y_2 - y_1)\}}{\{(x_2 - x_1)(y_3 - y_1) - (x_3 - x_1)(y_2 - y_1)\}}$$

$$a_2 = \frac{\{(u_3 - u_1)(x_2 - x_1) - (u_2 - u_1)(x_3 - x_1)\}}{\{(x_2 - x_1)(y_3 - y_1) - (x_3 - x_1)(y_2 - y_1)\}}$$

Similar expressions obtain for b_0 , b_1 and b_2 in terms of v , and for c_0 , c_1 , and c_2 in terms of q , respectively, in place of u in the above equations. The calculations have been carried out using a program written for the Olivetti "Programma 101" by Mr. L.D. Williams.

*Personal communication, 1961.

Bannon, Matthewman and Murray (1961) obtained comparable results for monthly averages by the triangulation and the grid methods over areas of $0.3 - 0.8 \times 10^5 \text{ km}^2$ in the British Isles, although Barry (1968) found less satisfactory agreement over an area of $1.4 \times 10^5 \text{ km}^2$ in southeast Labrador-Ungava. Hutchings (1957) obtained good results for a three-month period over an area of $0.9 \times 10^5 \text{ km}^2$ in southern England, however; and Rasmusson (1970) used a polygonal area of $2.6 \times 10^5 \text{ km}^2$ in the Upper Colorado river basin.

The triangles selected in the present study are those formed by the stations at the vertices Frobisher Bay - Clyde - Hall Beach ($1.9 \times 10^5 \text{ km}^2$), Egedesminde - Clyde - Frobisher Bay ($2.25 \times 10^5 \text{ km}^2$) and Egedesminde - Thule - Clyde ($1.87 \times 10^5 \text{ km}^2$). These triangles are shown in Figure 21. Station locations and elevations are listed in Appendix 1. The flux divergence analysis for Frobisher - Clyde - Hall Beach was determined at the surface, 950, 900, 850, 800, 700, 600 and 500 mbar levels, but for the other two triangles it was restricted, by the available data for Egedesminde, to the surface, 850, 700, 600 and 500 mbar levels. A modified Olivetti program for the vertical integration of the data was developed to deal with these cases. Vertical integration between the surface and 500 mbar was approximated by the trapezoidal rule using the following weights.

Level	Weight	Level	Weight
Surface	$[(P_s - 1000)/200] + 0.25$	Surface	$[(P_s - 1000)/200] + 0.75$
950 mbar	$[(P_s - 1000)/200] + 0.5$		
900	0.5		
850	0.5	850 mbar	$[(P_s - 1000)/200] + 1.5$
800	0.75		
700	1.0	700	1.25
600	1.0	600	1.0
500	0.3	500	0.5

P_s = surface pressure (mbar)

RESULTS

Flux Divergence

Figures 1-20 provide the basic results of the analysis of monthly flux divergence over the whole area.

In January the absolute magnitudes are small, generally within the range $\pm 4 \text{ g cm}^{-2} \text{ month}^{-1}$ in each of the five years. The gradients of the flux divergence isolines are also weak. (Note that the interval is 0.5 or $1.0 \text{ g cm}^{-2} \text{ month}^{-1}$.) In January 1961 and 1962 there was weak convergence over southern Baffin, in January 1965 over Baffin Bay and

most of Baffin Island, while in January 1963 and 1964 there was divergence extending from southern Greenland over much of Baffin Island.

In April the range of absolute values and the gradients of the isolines of flux divergence are somewhat greater. Over most of Baffin Island there was convergence of vapour flux in April 1961 and 1962, and divergence in 1963, 1964 and 1965.

The absolute magnitudes in July are within the range $\pm 30 \text{ g cm}^{-2} \text{ month}^{-1}$ with correspondingly large gradients. Convergence occurred over much of southern Baffin Island in each July, while northern Baffin Island had moderate divergence in 1963 and 1965. (The patterns further north are not considered here).

By October the magnitudes have decreased to approximately $\pm 10 \text{ g cm}^{-2} \text{ month}^{-1}$. In October 1963, 1964 and 1965 there was convergence over southern Baffin Island with divergence to the north. In October 1962 divergence covered much of the island while in 1961 there was divergence in the north and southwest, convergence in the southeast.

The mean patterns for January, April, and October 1961-65 are given in Figures 22-24. As is to be expected the January values are all close to zero. Weak convergence occurs over most of Baffin Island and particularly northeast Baffin Bay. The April values are also close to zero over Baffin Island with weak divergence to the north. Stronger convergence is now beginning to appear over the northern Labrador Sea. The general October pattern is somewhat similar but with much greater flux convergence in the south. The southern half of Baffin Island has flux convergence of $2-4 \text{ g cm}^{-2} \text{ month}^{-1}$. Figure 25 shows an average map combining January, April and October 1961-65, which can be taken as representative of the winter half-year.

The July map (Figure 26) shows strong flux convergence over southern Baffin Island-Foxe Basin and divergence over the Davis Strait-Hudson Strait area and over west Greenland. The sign of the divergence over northern Baffin Island accords with that determined separately for July 1961-65 over the Queen Elizabeth Islands (Barry, 1972)¹.

It is worth pointing out that the maps of flux divergence of vapour over North America prepared by Bock, Frazier, and Welsh (1966) for May 1958 – April 1963 show persistent convergence over north-central Baffin and divergence over southeast Baffin-Davis Strait. Such persistence, in most of the months they analyzed, seems

improbable and is more likely due to a combination of missing data, a smaller number of stations in this area and boundary effects at the edge of their grid network.

The computations for the three triangles are given in Tables 1-6. The arbitrary units of $10^{-5} \text{ g(cm}^2 \text{ 100 mbar sec)}^{-1}$ may be converted to $\text{g(cm}^2 \text{ 100 mbar month)}^{-1}$ by multiplying by 26.8×10^5 for a 31-day month and 25.9×10^5 for a 30-day month.

Comparison has been made of the two methods of analysis for the approximate (graphically estimated) centroids of the triangles – at 67.5°N , 72.5°W for Frobisher-Clyde-Hall Beach and at 67.5°N , 70°W for Egedesminde-Clyde-Frobisher (Table 7).

The correlation coefficients between the grid and triangle estimates are $+0.807$ for 67.5°N , 72.5°W and $+0.538$ for 67.5°N , 70°W . The second of these sets is outside the significant range, but the first is significant at $<1\%$ level. In view of the problem of reading values from the maps for the estimated centroid position and the sharp variations of flux divergence these correlations are encouraging.

As a measure of spatial coherence of the flux divergence, the correlation between pairs of triangles for the 20 months has been calculated. $r = +0.603$ (significant at the 1% level) for the triangles Frobisher – Clyde – Hall Beach and Egedesminde – Clyde – Frobisher, and $r = +0.840$ (significant at the 1% level) for Egedesminde – Clyde – Frobisher and Egedesminde – Thule – Clyde. This suggests less similarity between the southern half of Baffin Island and the Davis Strait area, than between Davis Strait and the eastern half of Baffin Bay. This point may merit further examination.

The vertical variation of flux divergence is shown for the mean values of January, April, July, and October, 1961-65 in Figures 27-30. These demonstrate a general similarity of vertical profile for each of the three triangles and they emphasize the problem of vertical sampling where data are available for only five levels. This is particularly serious in July, when much of the flux convergence occurs at 950-900 mbar. There is no general indication that convergence (or divergence) at low levels is balanced by divergence (or convergence) at higher levels, except perhaps in April. The apparent importance of low-level flux convergence over Baffin Bay and Davis Strait in October, before freeze-up is well advanced, deserves further specific study. Precipitation amounts are large at this time of year in southeastern Baffin Island.

Comparison of Flux Divergence of Water Vapour and Moisture Budget Data

Comparison of the computed flux divergence of water vapour $\nabla \cdot \vec{V}_q$, with the surface moisture budget is discussed next along the lines used by Barry (1968), Rasmusson (1968).

¹ Note that in the grid calculations of $\nabla \cdot \vec{V}_q$ in this report the $(\delta \cos \phi)$ term was inadvertently omitted. Recalculation shows that the magnitude and distribution of the flux-divergence averages is not greatly affected.

$$\Delta q + \nabla \cdot \vec{V}q = P - E$$

where Δq = change in storage of atmospheric vapour
 P = precipitation

The problem for the Baffin area is the total absence of any information on evaporation. Walmsley (1966) provides average estimates for Baffin Bay, but there are no comparable data for Baffin Island. Attention is therefore concentrated on January, April, and October when evaporation over the land is negligible. For Baffin Bay, the mean values of Walmsley are used as a first order-of-magnitude estimate. Rasmusson (1969, p. 732) notes that departures from normal of the space-time average evaporation over central and eastern North America in winter make only a small contribution to the departure of P-E (although this may not hold for smaller areas).

The following estimates (in mm) are made for the triangles Frobisher-Clyde-Hall Beach and also for grid-point 67.5°N, 75°W, using precipitation observations at Dewar Lakes, and for Egedesminde-Clyde-Frobisher and also grid-point 67.5°N, 65°W, using precipitation observations at Broughton Island (Table 8).

The correlation coefficients between P-E and flux convergence for the individual months are all outside the 5% significance level ($r = 0.51$). They are +0.418 for the Egedesminde-Clyde-Frobisher triangle and +0.181 for the comparable grid-point, +0.370 for the Frobisher-Clyde-Hall Beach triangle and +0.229 for the comparable grid-point. However, it is apparent that there is a marked improvement if five-year means are considered. The six averages (three months in both areas) using the grid points give $r = +0.796$ and using the triangle estimates $r = +0.665$.

Table 1. Monthly Flux Divergence of Water Vapour. Triangle: Frobisher-Clyde-Hall Beach ($1.9 \times 10^5 \text{ km}^2$).
 (Units: $10^{-5} \text{ g cm}^{-2} \text{ 100 mbar}^{-1} \text{ s}^{-1}$; Divergence positive)

		SFC	950	900	850	800	700	600	500
		mbar level							
January	1961	0.0066	0.0029	0.0109	0.0112	0.0122	0.0080	0.0054	0.0011
	1962	0.0145	0.0114	0.0067	0.0057	0.0075	0.0021	0.0016	0.0002
	1963	0.0057	0.0181	-0.0093	-0.0016	0.0009	0.0084	0.0143	0.0090
	1964	0.0005	0.0028	0.0028	-0.0022	-0.0001	0.0102	0.0133	0.0062
	1965	-0.0047	0.0046	-0.0081	-0.0118	-0.0024	0.0026	0.0066	0.0050
April	1961	0.0285	-0.0077	-0.0225	-0.0366	-0.0366	-0.0202	-0.0104	-0.0044
	1962	0.0189	0.0161	0.0026	-0.0184	-0.0170	-0.0014	0.0030	0.0053
	1963	0.0274	0.0347	0.0156	0.0169	0.0198	0.0138	0.0192	0.0100
	1964	0.0196	-0.0006	0.0014	-0.0047	0.0003	-0.0048	-0.0109	-0.0020
	1965	0.0126	0.0147	0.0052	0.0012	0.0037	0.0085	0.0049	0.0006
July	1961	0.0414	-0.0683	-0.0674	-0.0926	-0.0730	-0.0461	-0.0427	-0.0303
	1962	-0.0285	-0.1367	-0.0643	-0.0051	-0.0038	-0.0150	0.0001	0.0110
	1963	0.1001	0.0393	0.0314	0.0198	-0.0043	-0.0098	-0.0116	-0.0128
	1964	-0.1006	-0.2189	-0.1492	-0.1060	-0.1072	-0.0584	-0.0471	-0.0431
	1965	-0.0855	-0.1454	-0.1547	-0.1725	-0.1368	0.0100	0.0209	0.0189
October	1961	-0.0031	-0.0215	-0.0346	-0.0439	-0.0358	-0.0181	-0.0149	-0.0255
	1962	0.0461	-0.0171	-0.0054	-0.0000	-0.0030	0.0157	0.0214	0.0154
	1963	-0.0330	-0.0503	-0.0398	-0.0082	-0.0038	-0.0015	-0.0069	-0.0074
	1964	0.0139	-0.0061	-0.0162	-0.0112	0.0020	0.0180	0.0170	0.0119
	1965	-0.0245	-0.0268	-0.0134	-0.0074	-0.0021	0.0013	0.0090	0.0052
		MEAN VALUES							
		SFC	950	900	850	800	700	600	500
		mbar level							
Jan 1961-65		0.0074	-0.0011	0.0006	0.0003	0.0036	0.0063	0.0082	0.0043
April 1961-65		0.0214	0.0114	0.0005	-0.0083	-0.0060	-0.0008	-0.0012	0.0019
July 1961-65		-0.0146	-0.1060	-0.0808	-0.0713	-0.0650	-0.0200	-0.0161	-0.0113
Oct 1961-65		-0.0001	-0.0244	-0.0219	-0.0141	-0.0085	0.0031	-0.0051	-0.0001

Table 2. Monthly Flux Divergence of Water Vapour. Triangle: Egedesminde-Clyde-Frobisher ($2.25 \times 10^5 \text{ km}^2$).
(Units: $10^{-5} \text{ g cm}^{-2} 100 \text{ mbar}^{-1} \text{ s}^{-1}$; divergence positive)

		SFC	850	700	600	500
		mbar level				
January	1961	0.0219	-0.0159	-0.0154	-0.0156	-0.0105
	1962	0.0136	-0.0165	0.0015	0.0028	-0.0034
	1963	-0.1031	-0.0234	-0.0093	0.0070	0.0074
	1964	0.0392	-0.0059	0.0007	0.0087	0.0043
	1965	-0.0163	-0.0116	-0.0046	-0.0074	-0.0063
April	1961	0.0089	-0.0287	-0.0153	-0.0034	0.0008
	1962	0.0046	-0.0506	-0.0128	-0.0135	-0.0065
	1963	-0.0237	-0.0256	0.0061	0.0222	0.0180
	1964	0.0217	0.0023	-0.0025	-0.0002	0.0034
	1965	0.0245	0.0118	0.0164	0.0013	0.0045
July	1961	0.0297	-0.1117	-0.0938	-0.0567	-0.0272
	1962	0.0182	0.0670	0.0915	0.0810	0.0569
	1963	-0.0329	-0.0494	0.0362	0.0055	0.0155
	1964	-0.0392	-0.1912	-0.1401	-0.0940	-0.0397
	1965	-0.0600	0.0132	-0.0060	-0.0106	0.0026
October	1961	-0.0365	-0.0471	-0.0292	-0.0174	-0.0176
	1962	-0.0014	0.0044	0.0094	0.0137	0.0004
	1963	-0.0770	-0.0303	-0.0053	-0.0097	-0.0161
	1964	-0.1216	0.0087	0.0030	-0.0089	-0.0075
	1965	-0.0971	-0.0042	0.0004	0.0058	0.0082
		MEAN VALUES				
		SFC	850	700	600	500
		mbar level				
Jan 1961-65		-0.0081	-0.0147	-0.0054	-0.0009	-0.0017
April 1961-65		0.0072	-0.0182	-0.0016	0.0013	0.0040
July 1961-65		-0.0168	-0.0544	-0.0224	-0.0150	0.0016
Oct 1961-65		-0.0667	-0.0137	-0.0043	-0.0033	-0.0065

The former value is just outside the 5% significance level (0.811). The absolute magnitudes compare most closely for the Egedesminde-Clyde-Frobisher triangle, perhaps because orographic influences are less important. These results follow the findings of Rasmusson (1971), using nested regions of 42×10^5 to $5 \times 10^5 \text{ km}^2$, that the small areas give unreliable results on a monthly time scale.

CONCLUSIONS

The major findings of the investigation may be summarized briefly as follows:

1. the patterns of monthly flux divergence as analyzed by finite difference methods appear to be an improvement

over previous determinations (e.g., Bock *et al.*, 1966) in that there is no indication of recurring systematic errors. This is believed to be due to the estimations of missing data and the extension of the station network to include west Greenland.

2. the correlations between the triangle and grid computations of flux divergence are still not altogether satisfactory. Further work may be more profitably devoted to improving the grid methods by smoothing techniques.
3. the provisional work on moisture budget estimates suggests that the results are better over ocean areas perhaps because of the absence of topographic effects. The comparison for 5-year averages appears to produce useful results. On a monthly time scale the "noise" overrides the pattern.

Table 3. Monthly Flux Divergence of Water Vapour. Triangle: Egedesminde-Thule-Clyde ($1.87 \times 10^5 \text{ km}^2$).
(Units: $10^{-5} \text{ g cm}^{-2} 100 \text{ mbar}^{-1} \text{ s}^{-1}$; divergence positive)

		SFC	850	700	600	500
		mbar level				
January	1961	0.0124	-0.0237	-0.0379	-0.0308	-0.0194
	1962	-0.0521	-0.0250	-0.0075	-0.0022	-0.0043
	1963	-0.1013	-0.0336	-0.0126	-0.0149	-0.0055
	1964	-0.0131	-0.0258	-0.0179	-0.0193	-0.0148
	1965	-0.0396	-0.0193	-0.0299	-0.0351	-0.0210
April	1961	-0.0060	0.0207	0.0222	0.0221	0.0115
	1962	-0.0399	-0.0356	-0.0280	-0.0278	-0.0160
	1963	-0.0263	-0.0212	-0.0050	0.0010	0.0021
	1964	-0.0297	-0.0223	-0.0192	-0.0220	-0.0154
	1965	-0.0272	-0.0189	-0.0172	-0.0086	-0.0067
July	1961	-0.0343	-0.0912	-0.0770	-0.0326	-0.0210
	1962	0.0935	0.0102	0.0323	0.0404	0.0236
	1963	-0.0459	-0.0830	-0.0265	-0.0298	-0.0130
	1964	0.0122	-0.1337	-0.1345	-0.0878	-0.0406
	1965	0.0714	0.0226	-0.1056	-0.0850	-0.0464
October	1961	-0.1215	0.0146	0.0007	0.0050	0.0042
	1962	-0.0669	0.0085	-0.0166	-0.0193	-0.0148
	1963	-0.0828	-0.0170	-0.0047	-0.0043	-0.0044
	1964	-0.1029	0.0148	-0.0004	-0.0146	-0.0191
	1965	-0.1195	-0.0350	-0.0249	-0.0335	-0.0175
		MEAN VALUES				
		SFC	850	700	600	500
		mb level				
Jan 1961-65		-0.0387	-0.0255	-0.0212	-0.0205	-0.0130
April 1961-65		-0.0258	-0.0155	-0.0094	-0.0071	-0.0049
July 1961-65		0.0194	-0.0550	-0.0623	-0.0390	-0.0195
Oct 1961-65		-0.0937	-0.0028	-0.0092	-0.0133	-0.0103

Table 4. Monthly Flux Divergence of Water Vapour. Triangle: Frobisher-Clyde-Hall Beach
($1.9 \times 10^5 \text{ km}^2$)
(Units: $\text{g cm}^{-2} \text{ month}^{-1}$, divergence positive)

	Jan.	April	July	Oct.
1961	1.01	-2.19	-7.08	-3.34
1962	0.68	-0.04	-3.59	1.18
1963	0.38	2.57	1.78	-1.96
1964	0.76	-0.31	-12.84	0.79
1965	-0.11	0.84	-8.91	-0.53
	MEAN			
1961-65	0.57	0.11	-6.16	-0.79

Table 5. Monthly Flux Divergence of Water Vapour. Triangle: Egedesminde-Clyde-Frobisher
($2.25 \times 10^5 \text{ km}^2$)
(Units: $\text{g cm}^{-2} \text{ month}^{-1}$, divergence positive)

	Jan.	April	July	Oct.
1961	-1.27	-1.56	-9.02	-4.41
1962	-0.31	-2.78	9.21	0.84
1963	-3.17	-0.05	-1.19	-3.38
1964	0.87	0.51	-16.31	-2.39
1965	-1.24	1.61	-1.19	-1.88
	MEAN			
1961-65	-0.99	-0.55	-3.74	-2.24

Table 6. Monthly Flux Divergence of Water Vapour. Triangle:
Egedesminde-Thule-Clyde
($1.87 \times 10^5 \text{ km}^2$)
(Units: $\text{g cm}^{-2} \text{ month}^{-1}$, divergence positive)

	Jan.	April	July	Oct.
1961	-3.06	2.17	-8.26	-1.67
1962	-2.37	-4.09	4.98	-2.29
1963	-4.48	-1.55	-6.33	-2.67
1964	-2.63	-2.93	-12.58	-2.22
1965	-3.84	-2.27	-3.96	-5.88
	MEAN			
1961-65	-3.25	-1.72	-5.26	-2.94

Table 7. Comparison of Grid and Triangle Estimates of Vapour-Flux Divergence.

		Frobisher-Clyde-Hall Beach		Egedesminde-Clyde-Frobisher	
		Grid 67.5°N, 72.5°W	Centroid of Triangle	Grid 67.5°N, 70°W	Centroid of Triangle
July	1961	-5.4	-7.1	-10.3	-9.0
	1962	-7.9	-3.6	-4.0	9.2
	1963	-2.4	1.8	-2.3	-1.2
	1964	-8.2	-12.8	-8.3	-16.3
	1965	-6.3	-8.9	-6.4	-1.2
Oct.	1961	-2.6	-3.3	-6.1	-4.4
	1962	1.0	1.2	3.5	0.8
	1963	-2.7	-2.0	-3.5	-3.4
	1964	0.5	0.8	0.4	-2.4
	1965	-3.7	-0.5	-2.6	-1.9

Table 8. Comparison of Moisture Budget and Flux Convergence Estimates.

Egedesminde-Clyde-Frobisher							Frobisher-Clyde-Hall Beach				
P			E	P-E	Flux-convergence		P	E	P-E	Flux-convergence	
					Triangle	Grid				Triangle	Grid
Jan	1961	tr	0	0	13	32	tr	0	0	-10	3
	1962	0.8	0	1	3	7	tr	0	0	-7	5
	1963	75.7	0	76	32	25	19.3	0	19	-4	17
	1964	2.8	0	3	-9	-8	0	0	0	-8	8
	1965	10.7	0	11	12	16	6.6	0	7	11	5
Jan	1961-5			18	9.9	14.4			5	5.7	7.2
Apr	1961	22.8	0	23	16	39	tr	0	0	22	31
	1962	15.2	0	15	28	33	2.5	0	3	0	2
	1963	26.7	0	27	1	29	20.6	0	21	-26	5
	1964	4.6	0	5	-5	-13	6.1	0	6	3	-32
	1965	6.9	0	7	-16	-28	3.7	0	4	-8	12
Apr	1961-5			15	5.5	12.0			7	-1.1	3.6
Oct	1961	78.8	49	30	44	78	77.7	0	78	33	-10
	1962	22.0	49	-27	-8	-25	21.8	0	22	-12	15
	1963	44.9	49	-4	34	39	11.9	0	12	20	19
	1964	166.8	49	118	24	6	16.8	0	17	-8	-6
	1965	55.2	49	6	19	17	9.8	0	10	5	48
Oct	1961-5			25	22.4	23.0			28	7.9	13.2

REFERENCES

Bannon, J.K., Matthewman A. G. and Murray, R. 1961. The flux of water vapour due to the mean winds and the convergence of this flux over the northern hemisphere in January and July. *Quart. J. R. Met. Soc.* 87: 502-512.

Barry, R. G. 1968. Vapour flux divergence and moisture budget calculations for Labrador-Ungava. *Cah. Geogr. de Québec* 12(25): 91-102.

Barry, R. G. 1972. The summer flux divergence of atmospheric water vapour over the Queen Elizabeth Islands, N.W.T. McGill Univ. *Pub. in Met.*: 104. Montreal, 24 pp.

- Barry, R. G. and Fogarasi, S. 1968. Climatological studies of Baffin Island, N.W.T. *Tech. Bull. No. 13*. Inland Waters Branch, Ottawa. 106 pp.
- Bellamy, J. C. 1949. Objective calculations of divergence, vertical velocity and vorticity. *Bull. Am. Met. Soc.* 30: 45-49.
- Bock, P., Frazier, H. M. and Welsh, J. G. 1966. Moisture flux over North America. Part II. Analysis of monthly and longer term means of the flux divergence of moisture over Northern America, May 1958 – April 1963. Final Report, Contract CWb-11313, Travelers Research Center, Inc., Hartford, Conn. 97 pp.
- Brock, E. B. 1968. Daily divergence of water vapour transport. Unpublished S. M. Thesis, Meteorology Dept., M.I.T., Mass., 99 pp.
- Hutchings, J. W. 1957. Water vapour flux and flux divergence over southern England. Summer 1954. *Quart. J. R. Met. Soc.* 83: 30-48.
- Peixoto, J. P. 1970. Pole to pole divergence of water vapour. *Tellus* 22: 17-25.
- Rasmussen, J. L. 1970. Atmospheric water balance and hydrology of the upper Colorado River Basin. *Water Resources Res.* 6: 62-76.
- Rasmusson, E. M. 1967. Atmospheric water vapour transport and the water balance of North America: Part I. Characteristics of the water vapour flux field; *Mon. Wea. Rev.* 95, 403-426.
- Rasmusson, E. M. 1968. Part II. Large-scale water balance investigations. *Mon. Wea. Rev.* 96: 720-734.
- Rasmusson, E. M. 1971. A study of the hydrology of eastern North America using atmospheric flux data. *Mon. Wea. Rev.* 99: 119-135.
- Walmsley, J. L. 1966. Ice cover and surface heat fluxes in Baffin Bay. *Publication in Meteorology* No. 84:94 p. McGill University, Montreal.

Figures 1-30

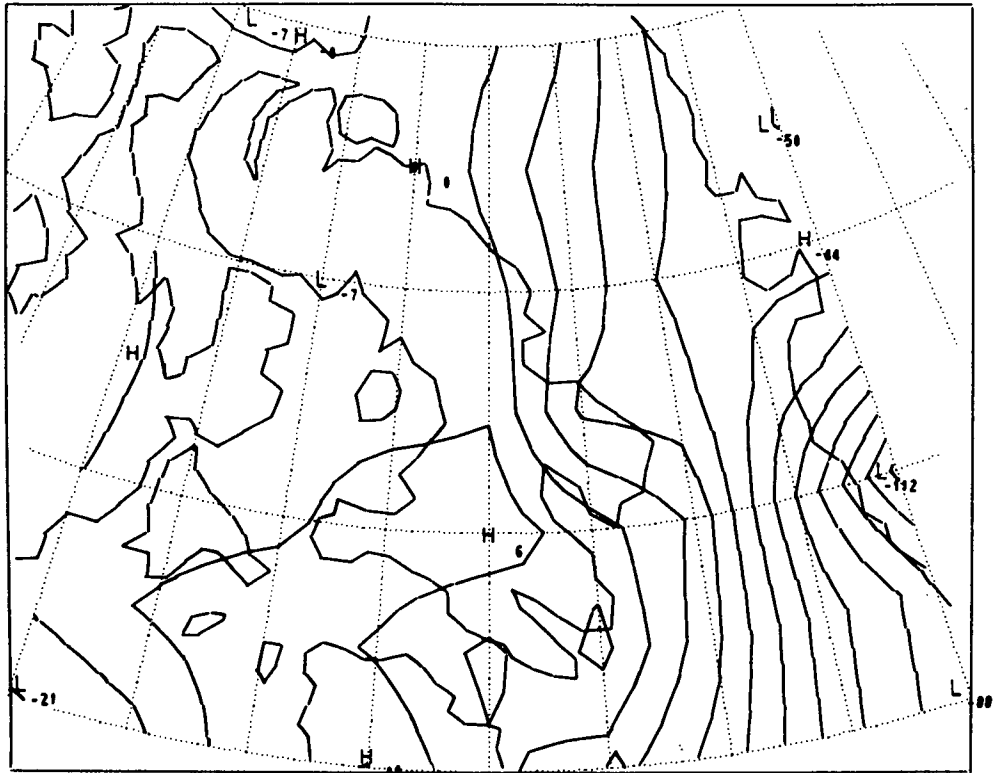


Figure 1. Flux divergence, January 1961. Contour from -12.00 to 2.00, Contour interval 1.00.

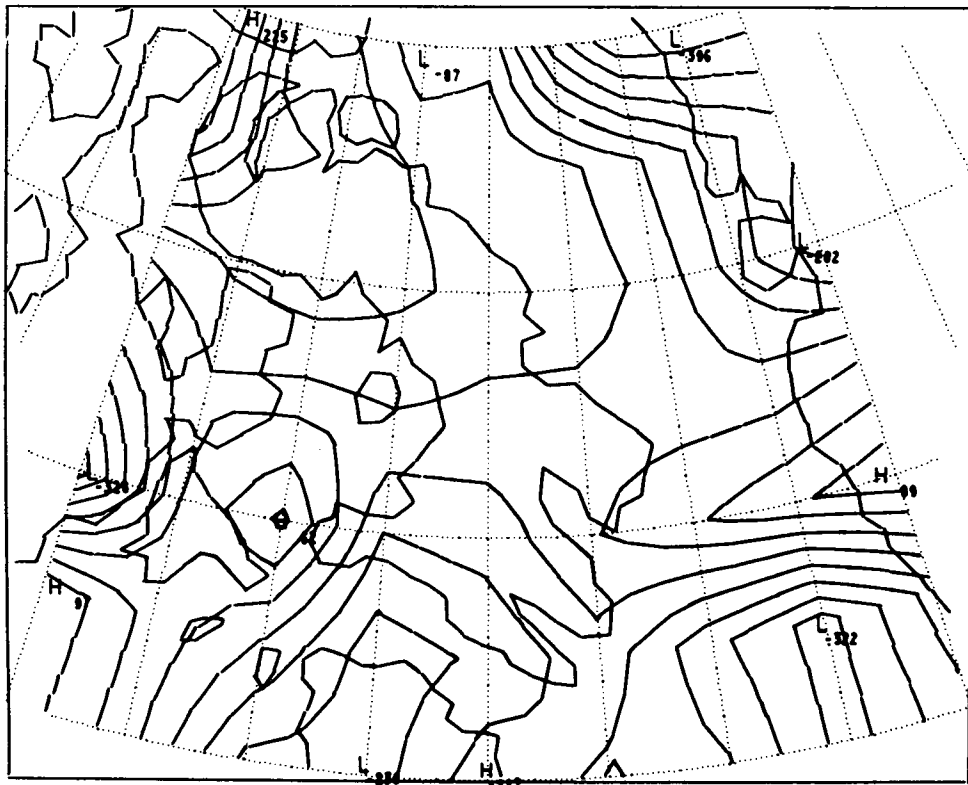


Figure 2. Flux divergence, January 1962. Contour from -4.00 to 2.50, Contour interval 0.50.

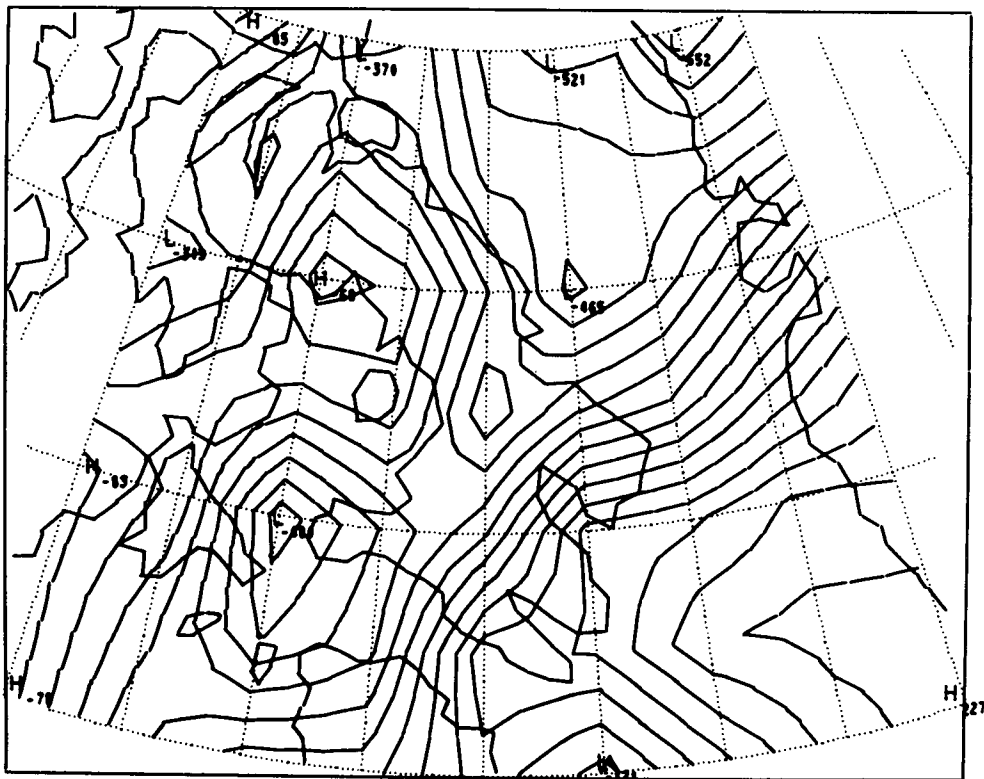


Figure 3. Flux divergence, January 1963. Contour from -7.00 to 2.50 , Contour interval 0.50 .

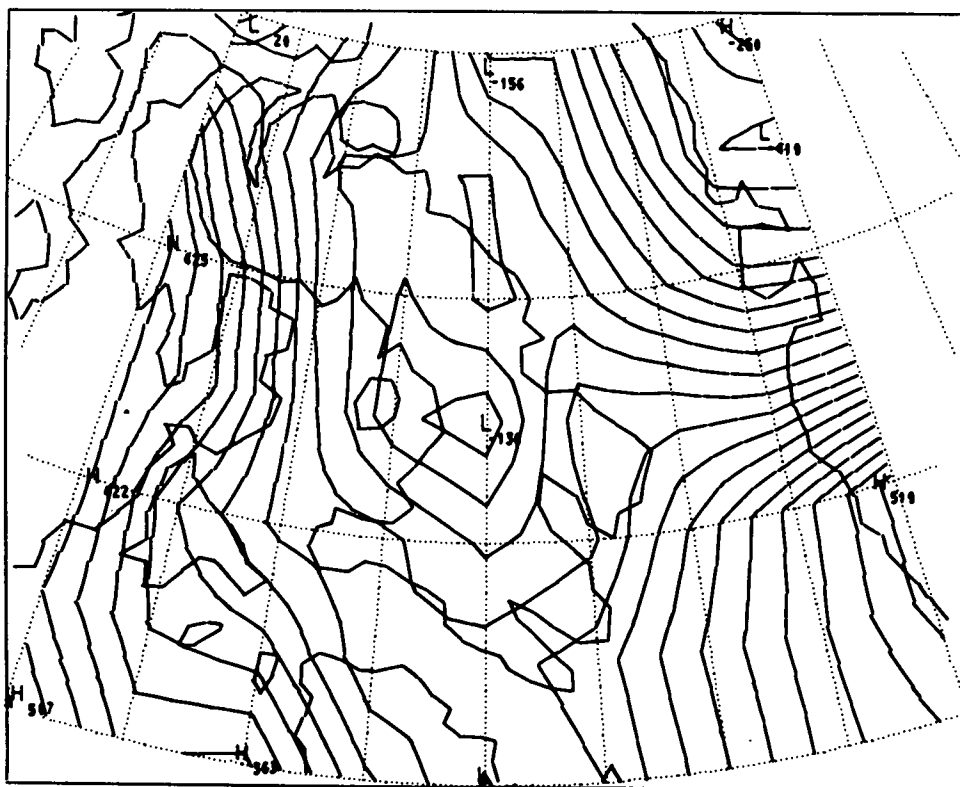


Figure 4. Flux divergence, January 1964. Contour from -4.50 to 5.50 , Contour interval 0.50 .

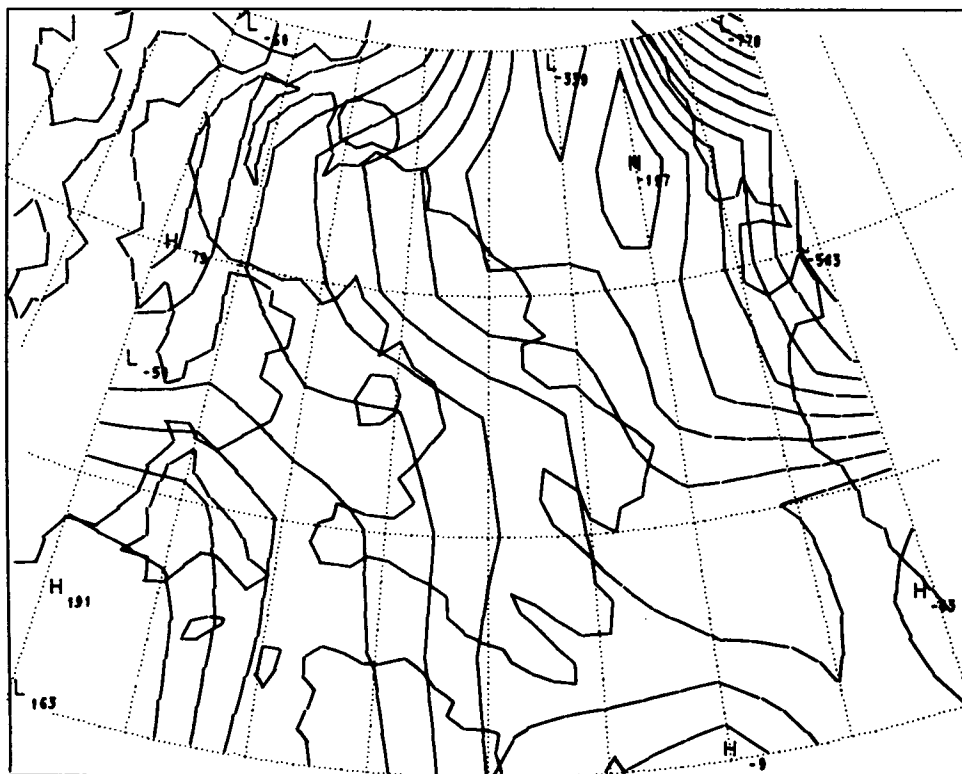


Figure 5. Flux divergence, January 1965. Contour from -8.00 to 2.00, Contour interval 0.50.

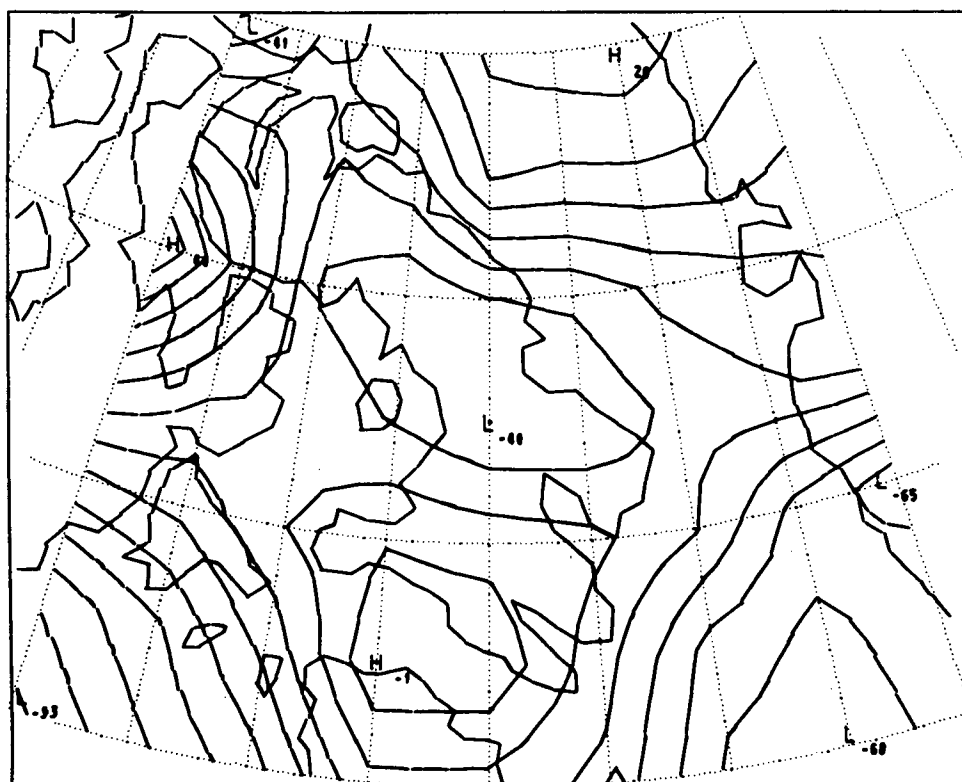


Figure 6. Flux divergence, April 1961. Contour from -10.00 to 5.00, Contour interval 1.00.

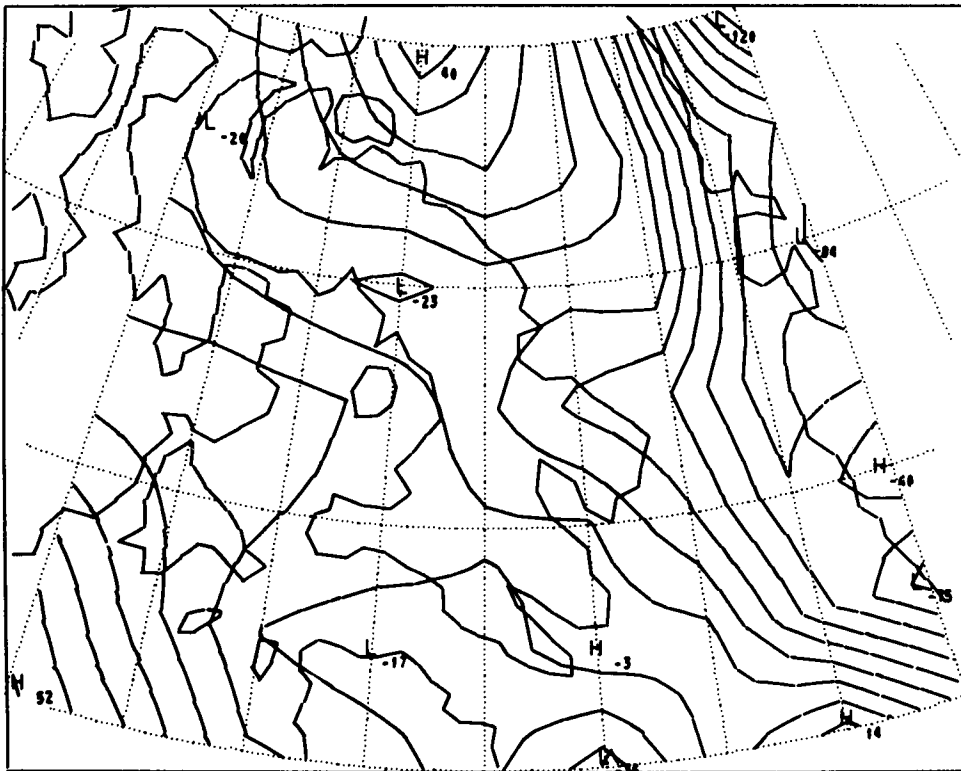


Figure 7. Flux divergence, April 1962. Contour from -15.00 to 6.00, Contour interval 1.00.

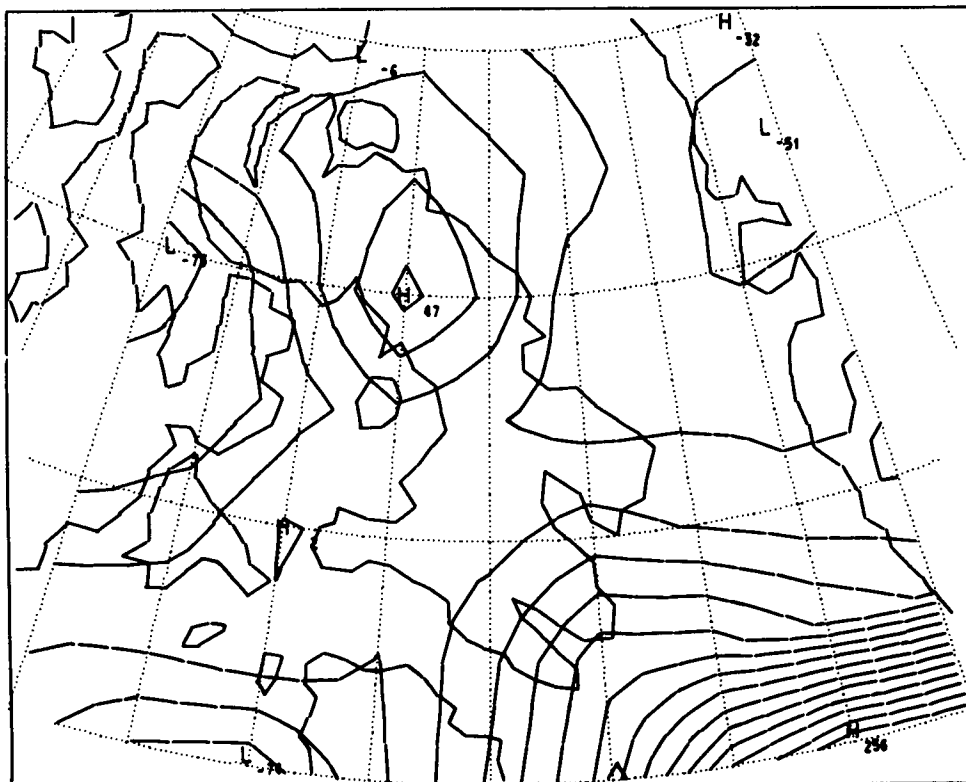


Figure 8. Flux divergence, April 1963. Contour from -8.00 to 26.00, Contour interval 2.00.

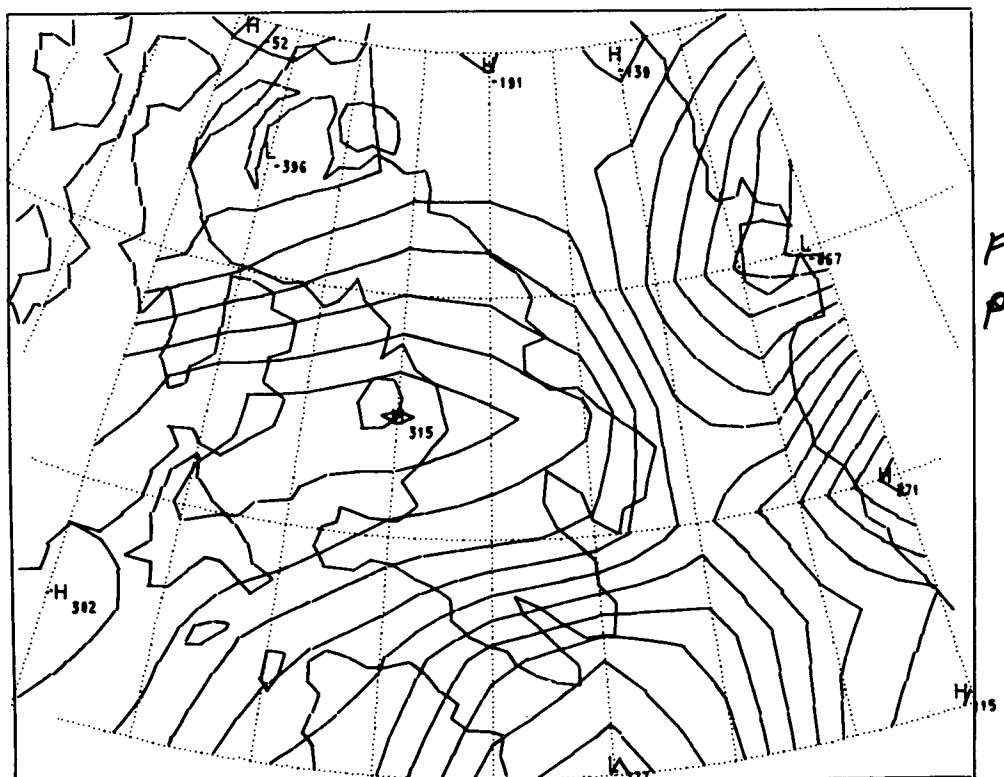


Figure 9. Flux divergence, April 1964. Contour from -9.00 to 4.00, Contour interval 1.00.

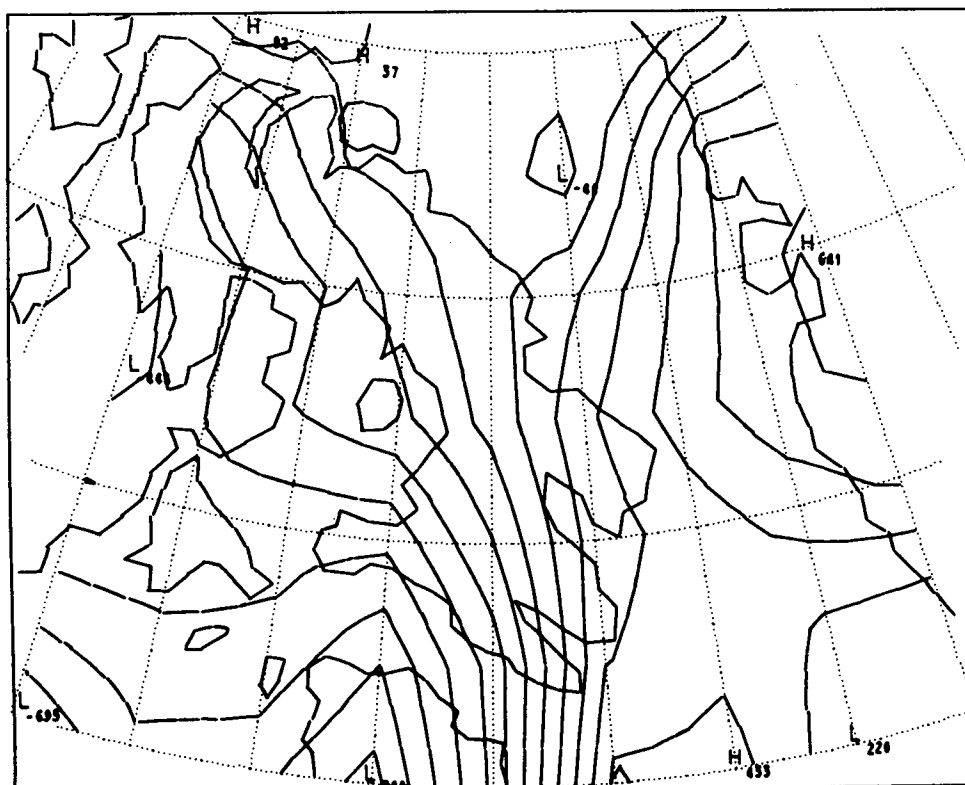


Figure 10. Flux divergence, April 1965. Contour from -8.00 to 7.00, Contour interval 1.00.

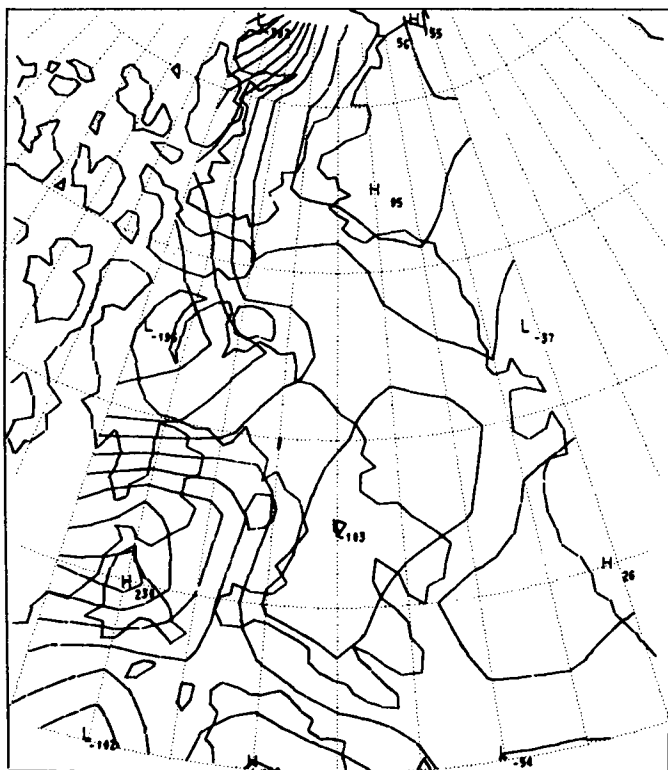


Figure 11. Flux divergence, July 1961. Contour from -40.00 to 25.00, Contour interval 5.00.

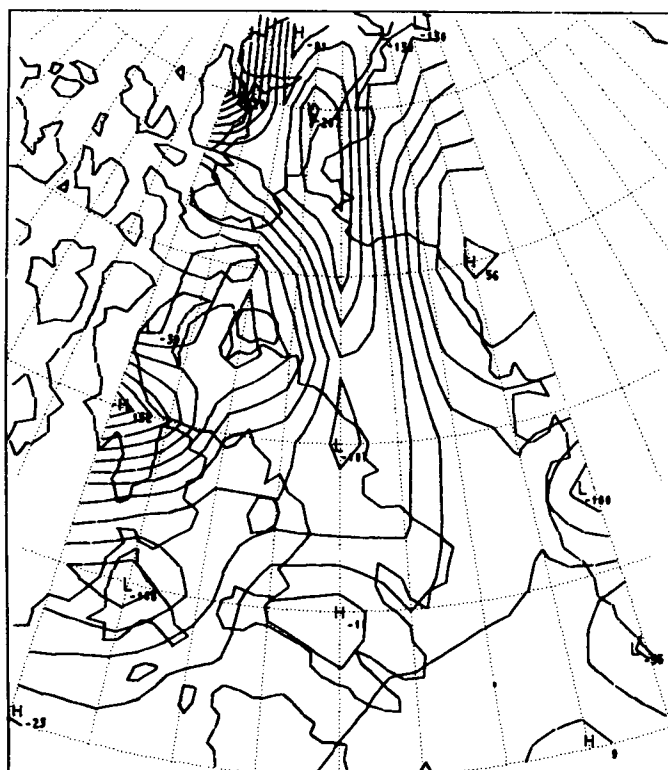


Figure 12. Flux divergence, July 1962. Contour from -25.00 to 25.00, Contour interval 2.50.

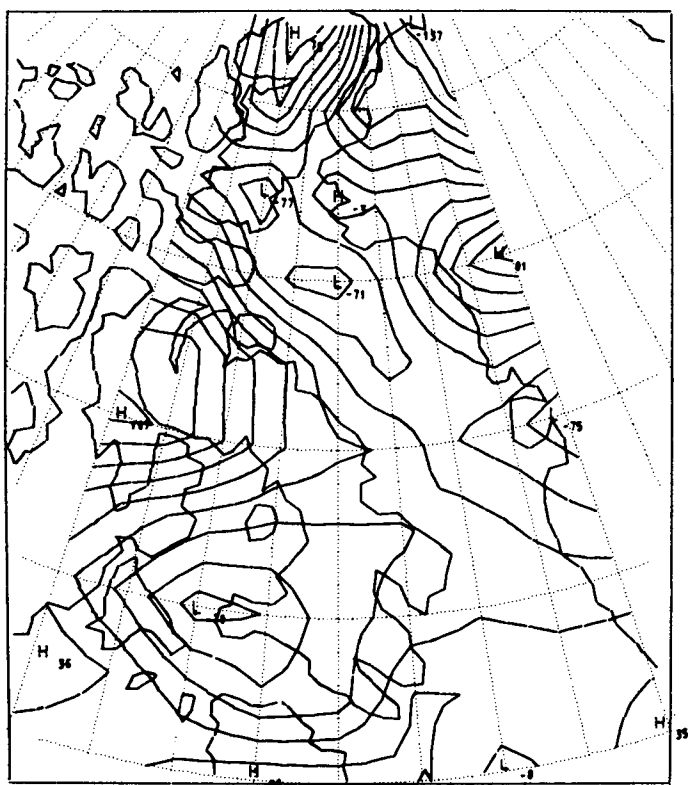


Figure 13. Flux divergence, July 1963. Contour from -14.00 to 12.00, Contour interval 2.00.

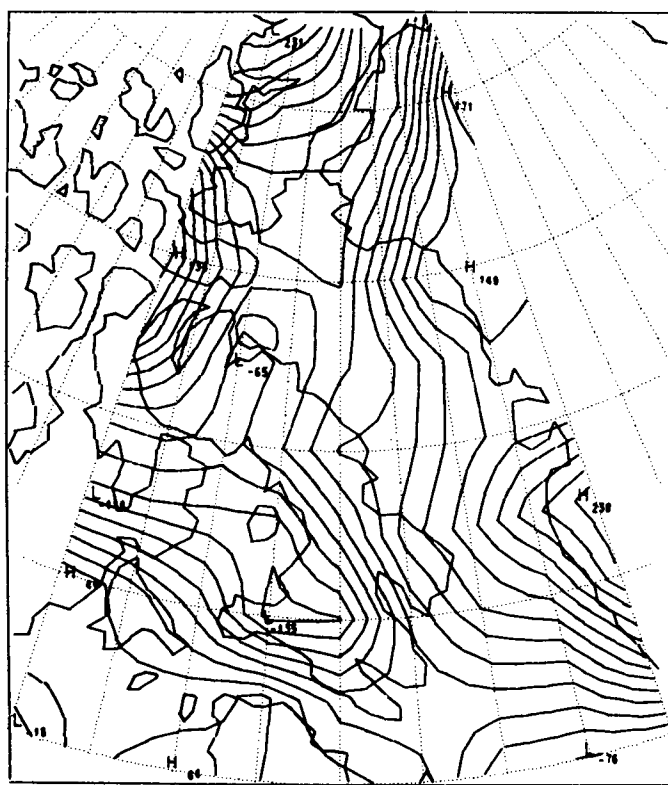


Figure 14. Flux divergence, July 1964. Contour from -35.00 to 20.00, Contour interval 2.50.

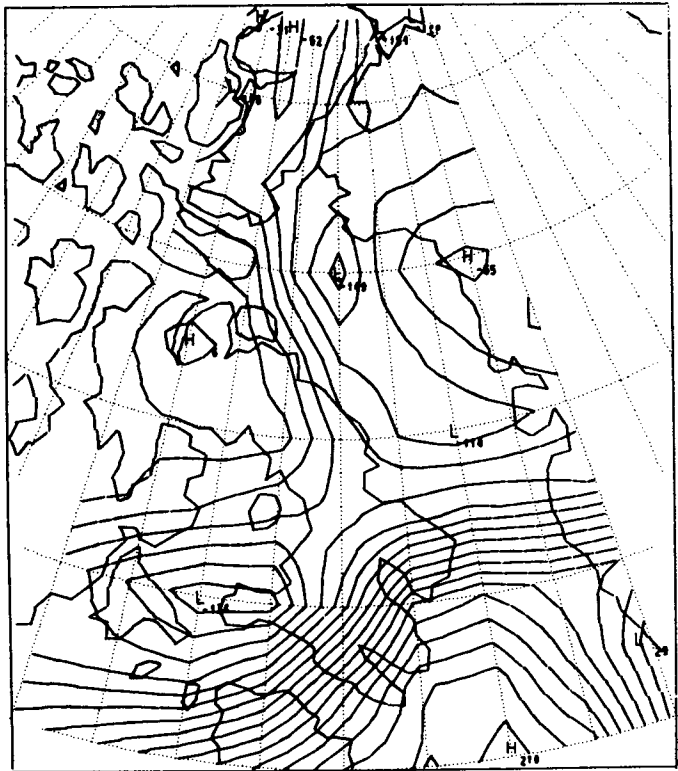


Figure 15. Flux divergence, July 1965. Contour from -16.00 to 22.00, Contour interval 2.00.

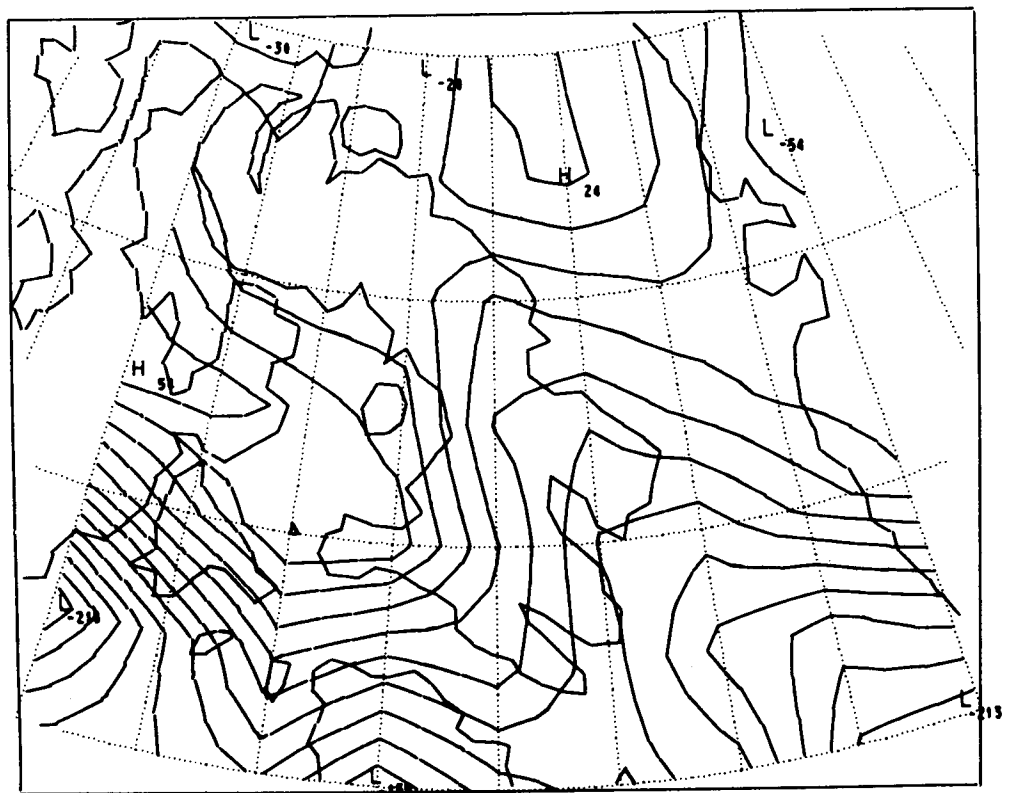


Figure 16. Flux divergence, October 1961. Contour from -22.00 to 6.00, Contour interval 2.00.

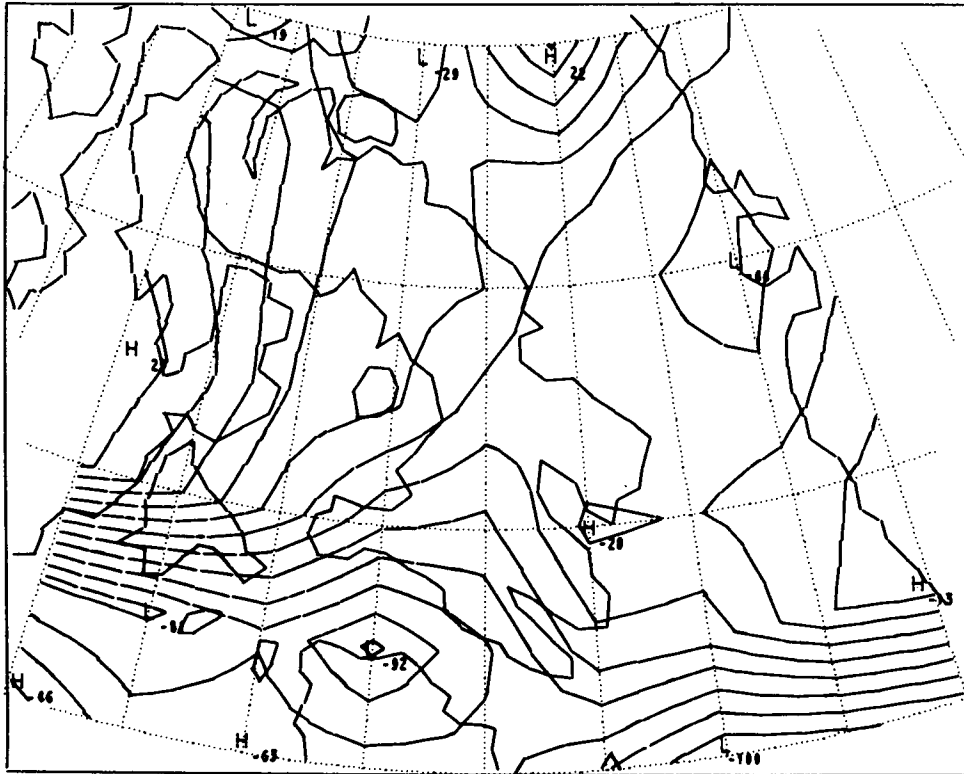


Figure 17. Flux divergence, October 1962. Contour from -35.00 to 10.00, Contour interval 2.50.

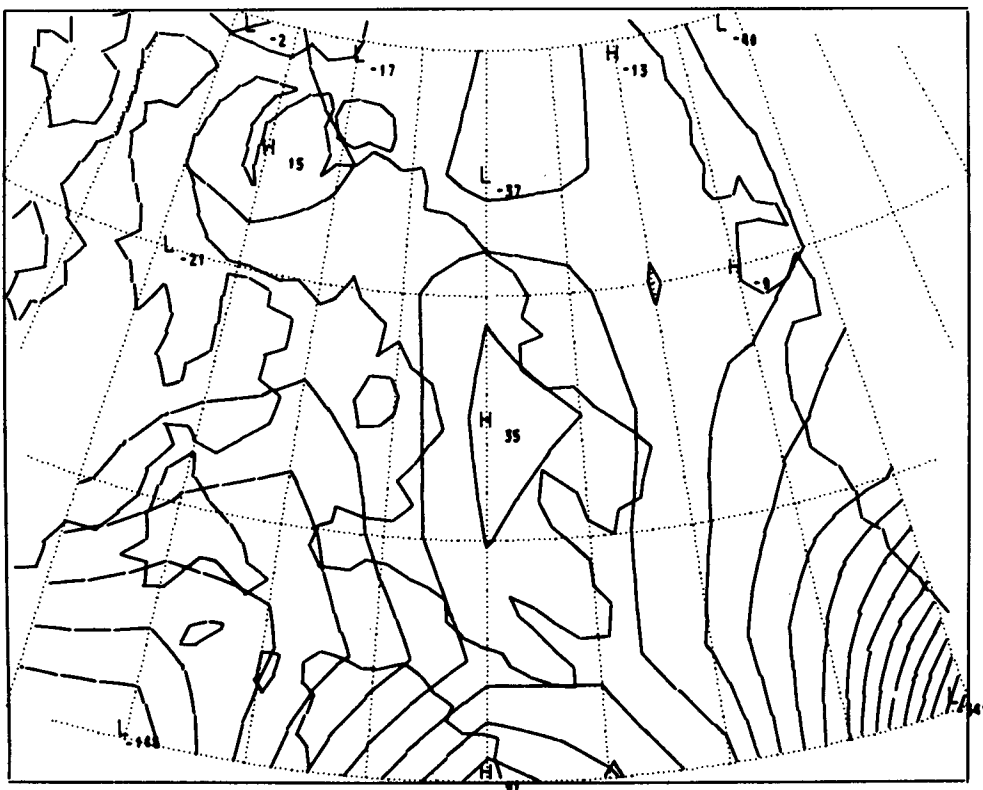


Figure 18. Flux divergence, October 1963. Contour from -10.00 to 3.00, Contour interval 1.00.

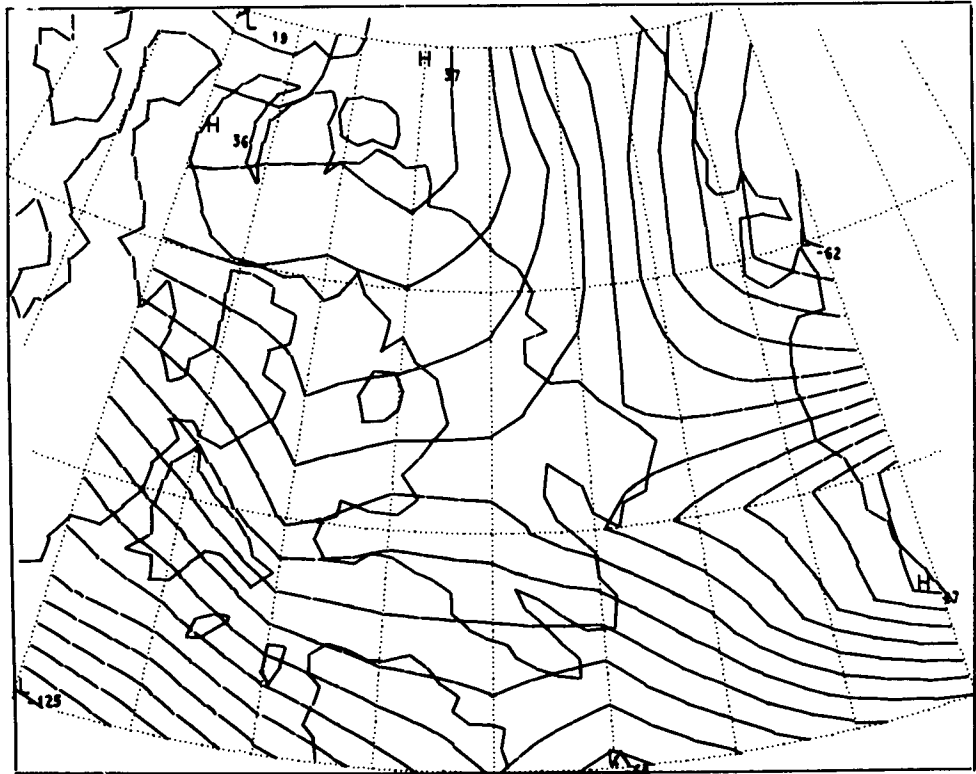


Figure 19. Flux divergence, October 1964. Contour from -13.00 to 5.00, Contour interval 1.00.

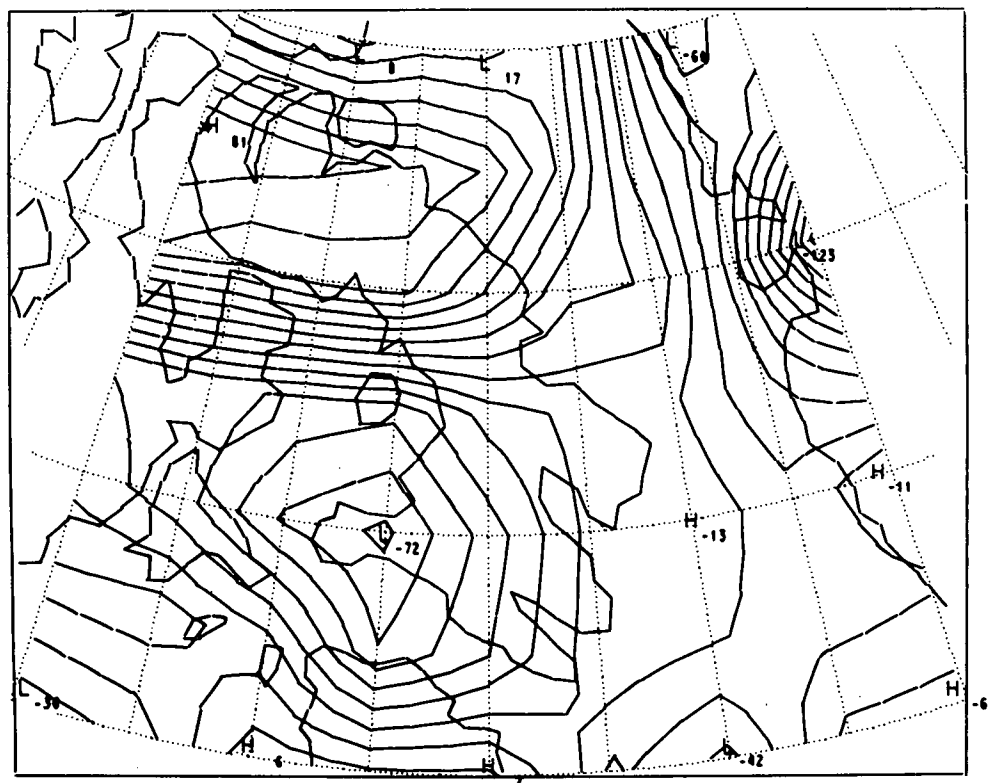


Figure 20. Flux divergence, October 1965. Contour from -14.00 to 10.00, Contour interval 1.00.

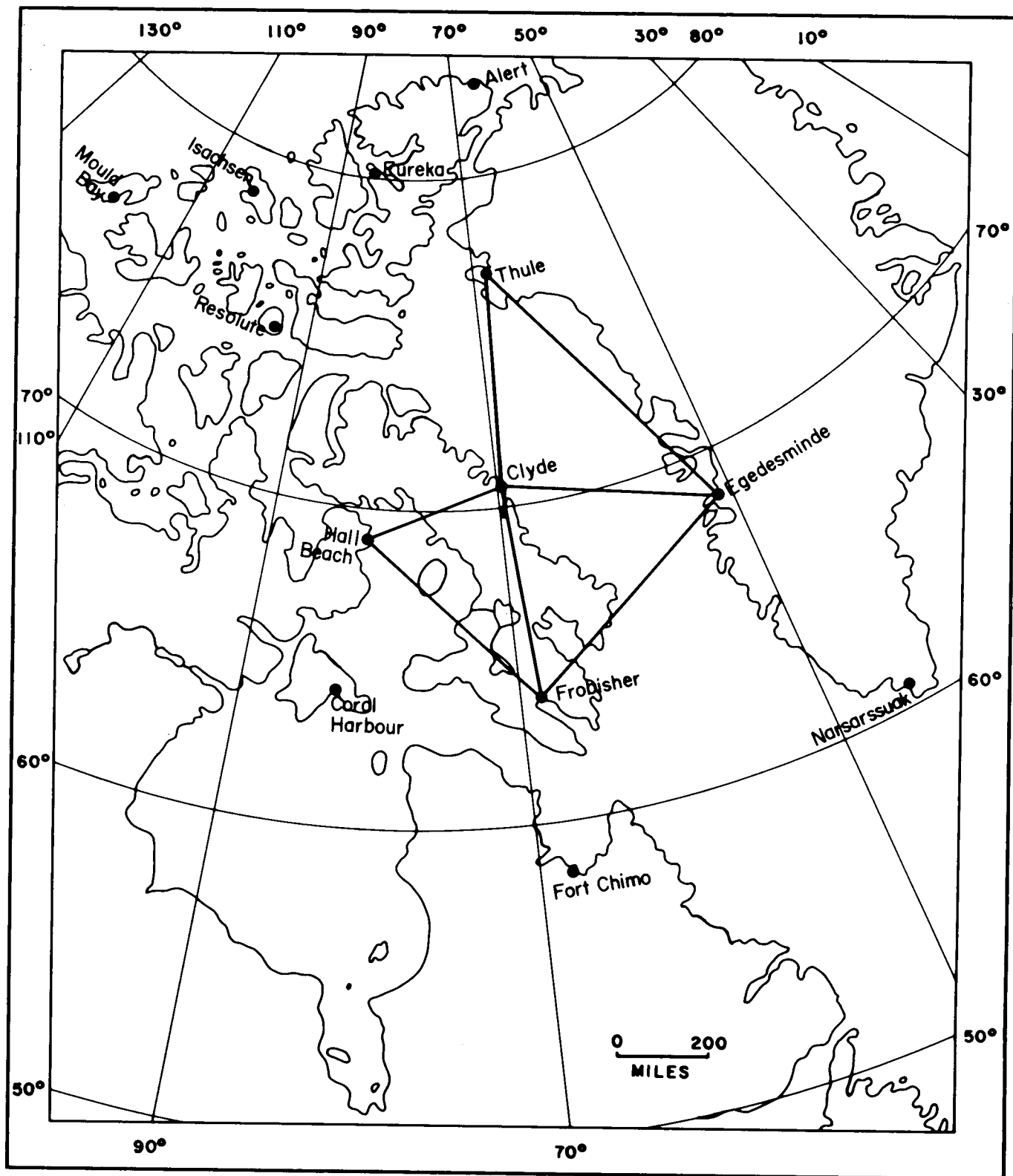


Figure 21. Rawinsonde stations and flux – divergence triangles.

Figure 22. Mean flux divergence, January 1961-65.

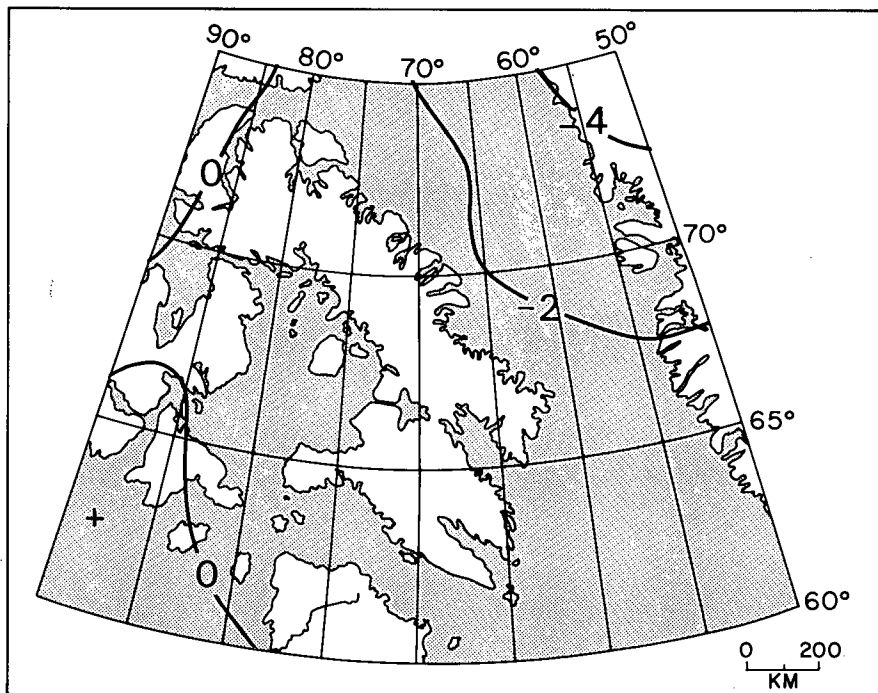
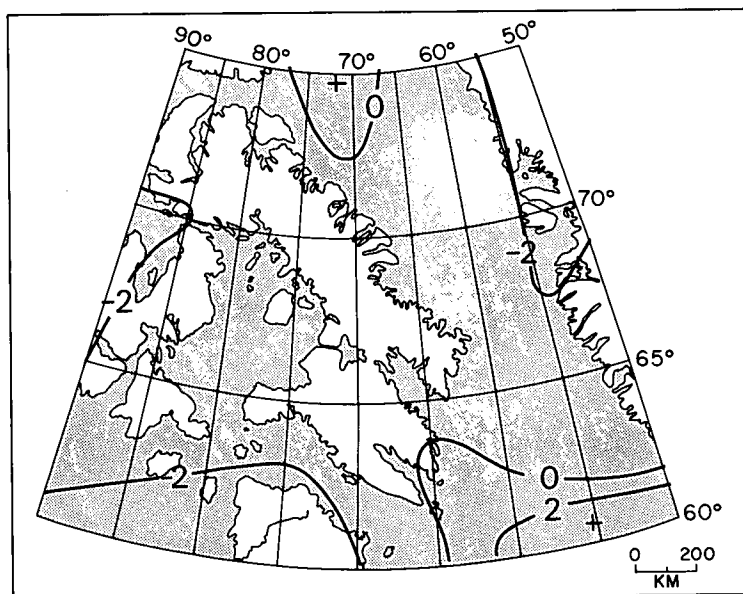


Figure 23. Mean flux divergence, April 1961-65.



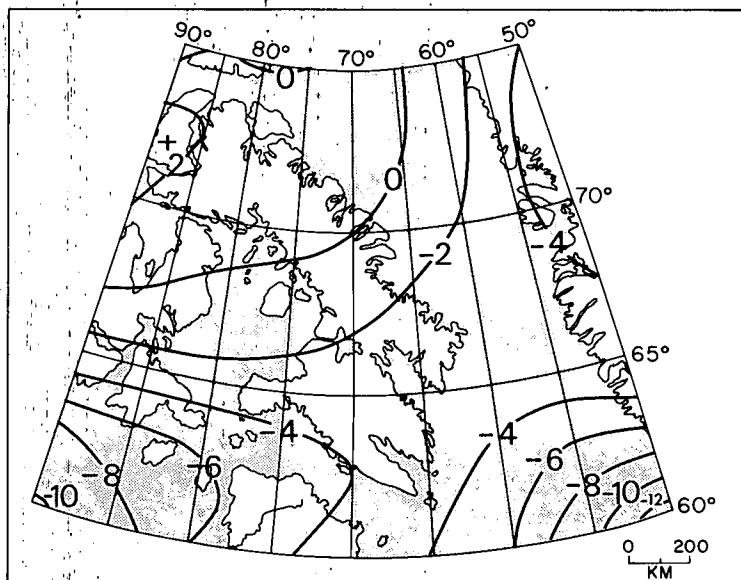


Figure 24. Mean flux divergence, October 1961-65.

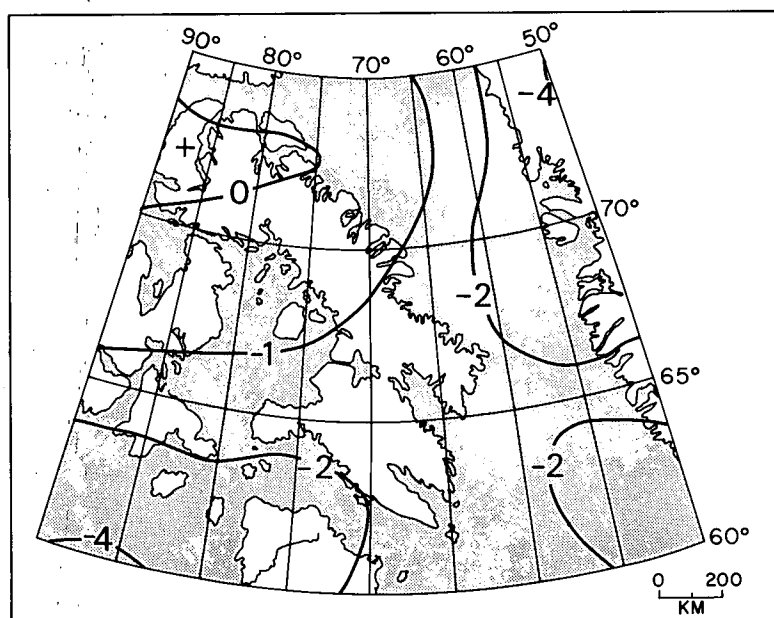


Figure 25. Mean flux divergence, mean winter season, 1961-65.

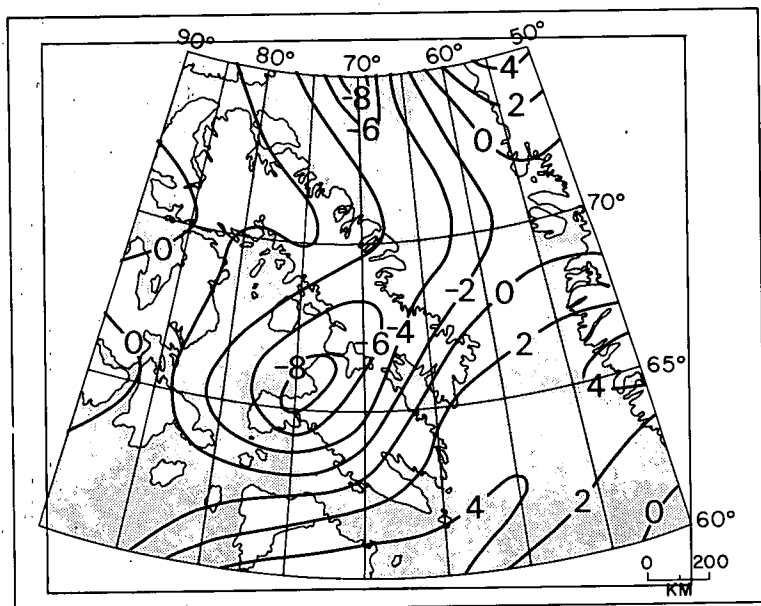


Figure 26. Mean flux divergence, July 1961-65.

x—x FROBISHER - CLYDE - HALL BEACH
 ●—● EGEDESMINDE - CLYDE - FROBISHER
 x--x EGEDESMINDE - THULE - CLYDE

JANUARY 1961-65

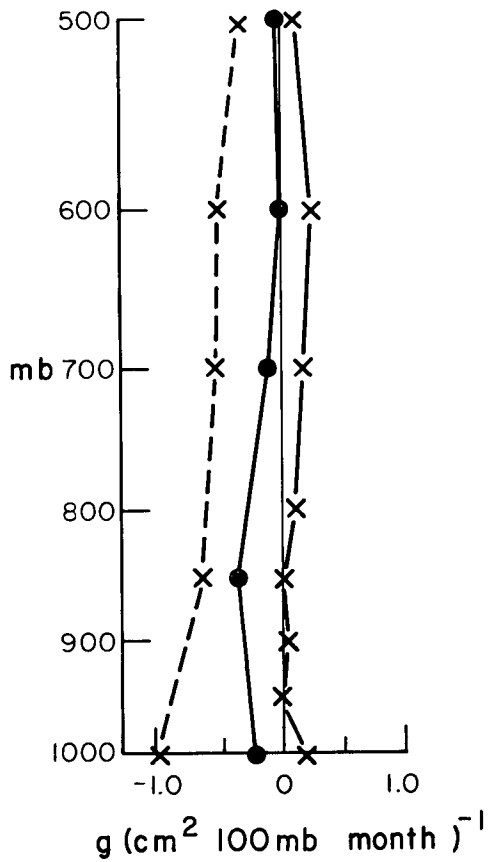


Figure 27. Profiles of flux divergence for selected triangles: Frobisher - Clyde - Hall Beach; Egedesminde-Clyde-Frobisher; Egedesminde-Thule-Clyde. January 1961-65.

APRIL 1961-65

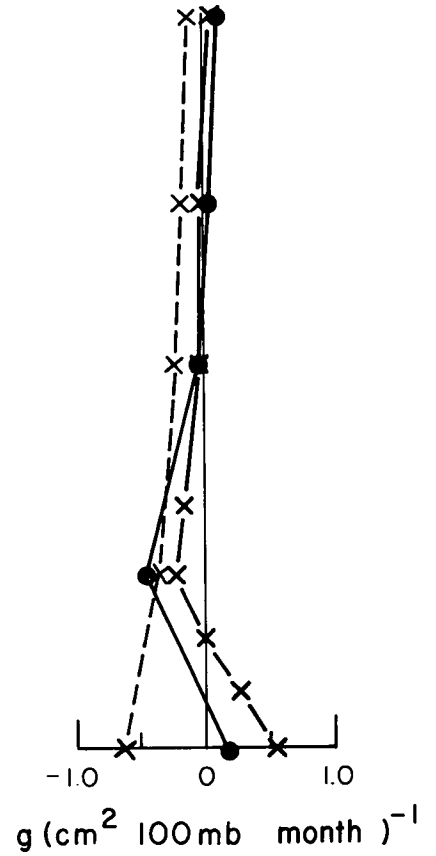


Figure 28. Profiles of flux divergence for selected triangles: Frobisher - Clyde - Hall Beach; Egedesminde-Clyde-Frobisher; Egedesminde-Thule-Clyde. April 1961-65.

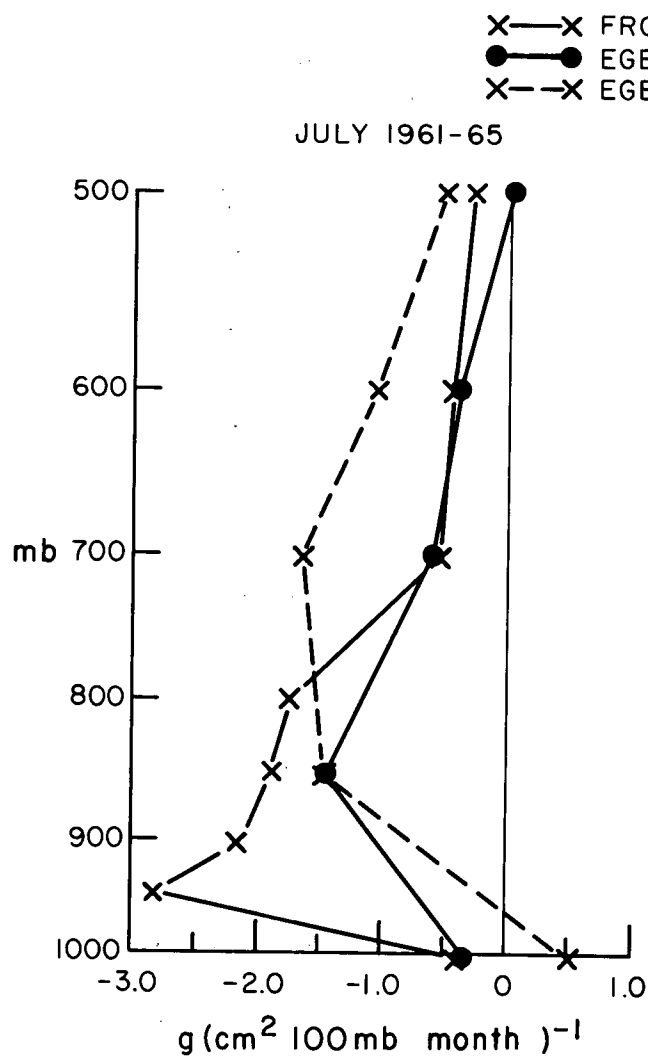


Figure 29. Profiles of flux divergence for selected triangles: Frobisher - Clyde - Hall Beach; Egedesminde-Clyde-Frobisher; Egedesminde-Thule-Clyde. July 1961-65.

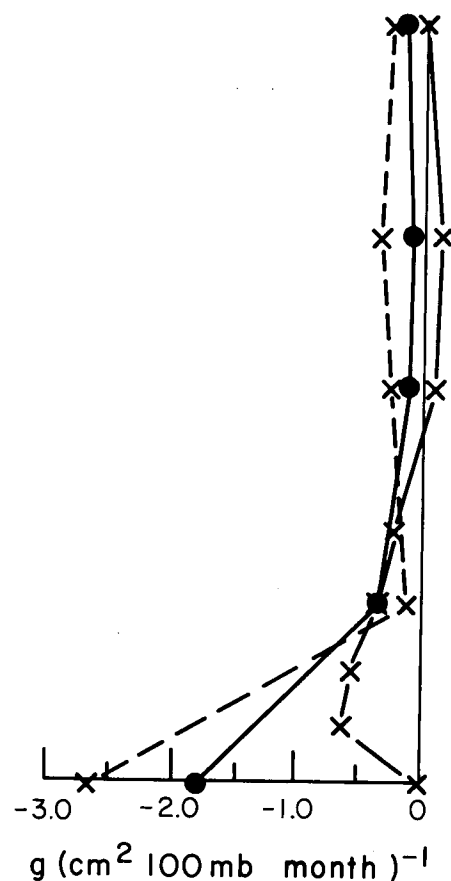


Figure 30. Profiles of flux divergence for selected triangles: Frobisher - Clyde - Hall Beach; Egedesminde-Clyde-Frobisher; Egedesminde-Thule-Clyde. October 1961-65.

APPENDIX 1

Stations for which Upper-Air Data Were Used in the Analysis

Station	Location	Elevation(m)	Comments
Alert	82.5°N,62.3°W	62	July 1961-5 only
Egedesminde	68.7°N,52.9°W	48	Data only available at 5 levels
Eureka	80.0°N,85.9°W	4	July 1961-5 only
Coral Harbour	64.2°N,83.4°W	59	
Clyde	70.5°N,68.6°W	16	
Fort Chimo	58.1°N,68.4°W	36	
Frobisher	63.8°N,68.6°W	21	
Hall Beach	68.8°N,81.3°W	10	
Isachsen	78.8°N 103.5°W	25	July 1961-5 only
Mould Bay	76.2°N,119.3°W	15	July 1961-5 only
Resolute	74.7°N,95.0°W	64	
Thule	76.5°N,68.8°W	11	

2. A Pressure Pattern Classification for Baffin Island

Contents

	Page
CLASSIFICATION OF PRESSURE AND CONTOUR PATTERNS	35
Background	35
Procedure	35
TYPE FREQUENCY	38
REFERENCES	38

Illustrations

Figure 1. Grid for pressure types	35
Figure 2. Schematic pressure types	36

Tables

1. Percentage frequency of MSL pressure — pattern types, 1961-65 and 1961-70 for July-August	38
--	----

A Pressure Pattern Classification for Baffin Island

CLASSIFICATION OF PRESSURE AND CONTOUR PATTERNS

Background

The classification of synoptic weather maps into types has a history of almost a century and since the various approaches have been viewed in the literature (Blüthgen, 1965; Barry, 1967), it is only necessary to make one or two pertinent comments here. First, we should note that any classification of weather maps is to a greater or lesser degree subjective. Even if objective numerical methods or grouping are employed, the criteria used to determine class boundaries must ultimately be chosen subjectively (for example see Lund, 1963). The essential purpose of a classification is to provide a convenient means of summarizing the complexities of the day-to-day weather patterns into a limited number of categories for purposes of relating particular weather parameters to the synoptic scale events. The extent to which a classification is useful in this regard is the primary measure as to how successful the grouping is. The classification procedure may focus on:

1. the static pressure field at a given time over a given area.
2. the airflow direction at a given time over a given area.
3. the airflow taking into account its direction over the previous day or so.
4. the large-scale (mid-tropospheric) "steering" of surface depressions and similar synoptic features, i.e., *Grosswetterlage*

The approach adopted here is the first one. This method has the advantage that there is less problem in defining the appropriate flow direction over such extensive area as Baffin Island. Also, the direction of airflow in the eastern Canadian Arctic is in general much less significant than is the case in the eastern Canadian Subarctic. The "steering" approach is also less meaningful in the area of study as it is the location of a mean tropospheric low or trough throughout the year (Hare, 1968).

Procedure

The classification was developed through a process of trial and error by applying provisional schematic patterns to a selection of winter and summer maps. It was estimated that some 75% of maps can be assigned to the designated

types with little difficulty, another 15% might be placed in more than one category without careful scrutiny, and the remainder show complex or weak patterns which are more or less unclassifiable. Nevertheless, all days have been assigned to one of the types.

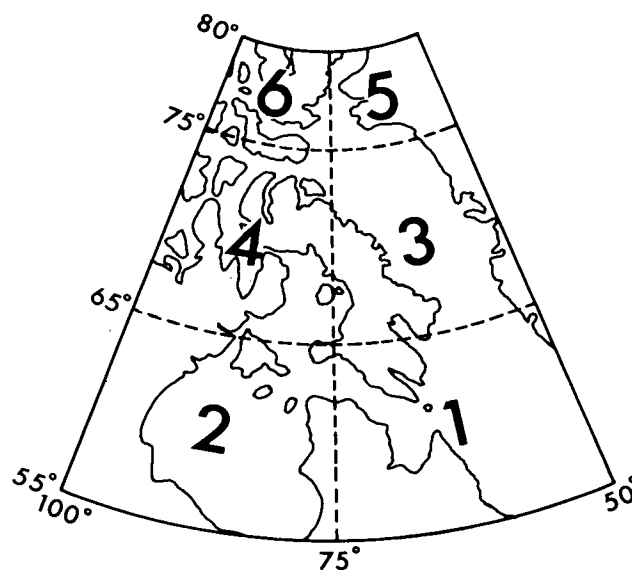


Figure 1. Grid for pressure types

The classification categories refer to the area delimited by latitudes 55° and 80°N and meridians 50° and 100°W (Fig. 1). The 41 surface types are shown schematically in Fig. 2. The three-figure reference coding operates as follows:

1. the hundreds digit designates nine basic patterns which refer to the location of high and low pressure centres.

- 1 = central low
- 2 = low to E, high to W
- 3 = low to S, high to N
- 4 = low to W, high to E
- 5 = Baffin Bay trough (and/or low to SE)
- 6 = low to SW
- 7 = low to NE, high to SW
- 8 = col
- 9 = anticyclonic

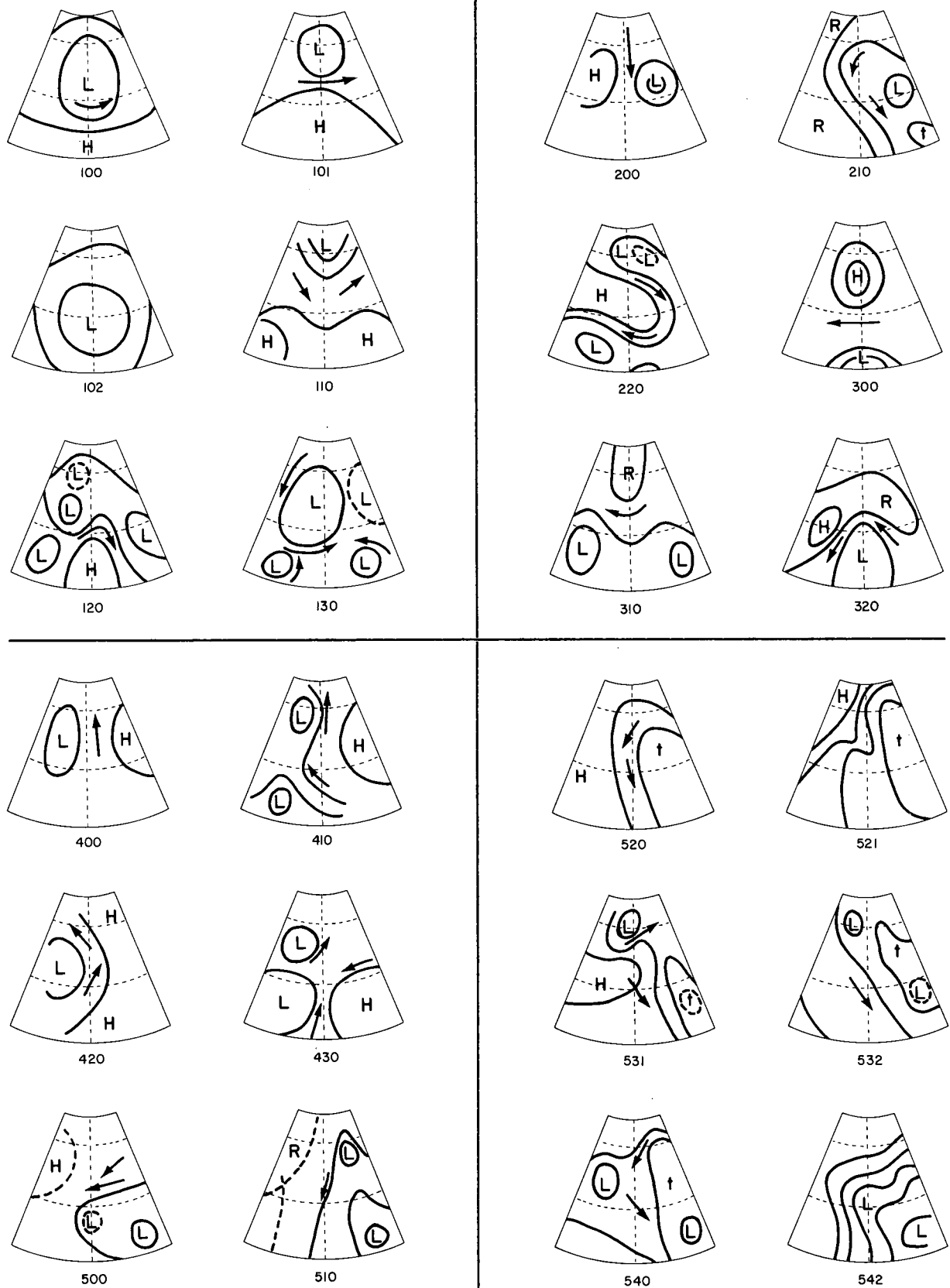


Figure 2. Schematic pressure types

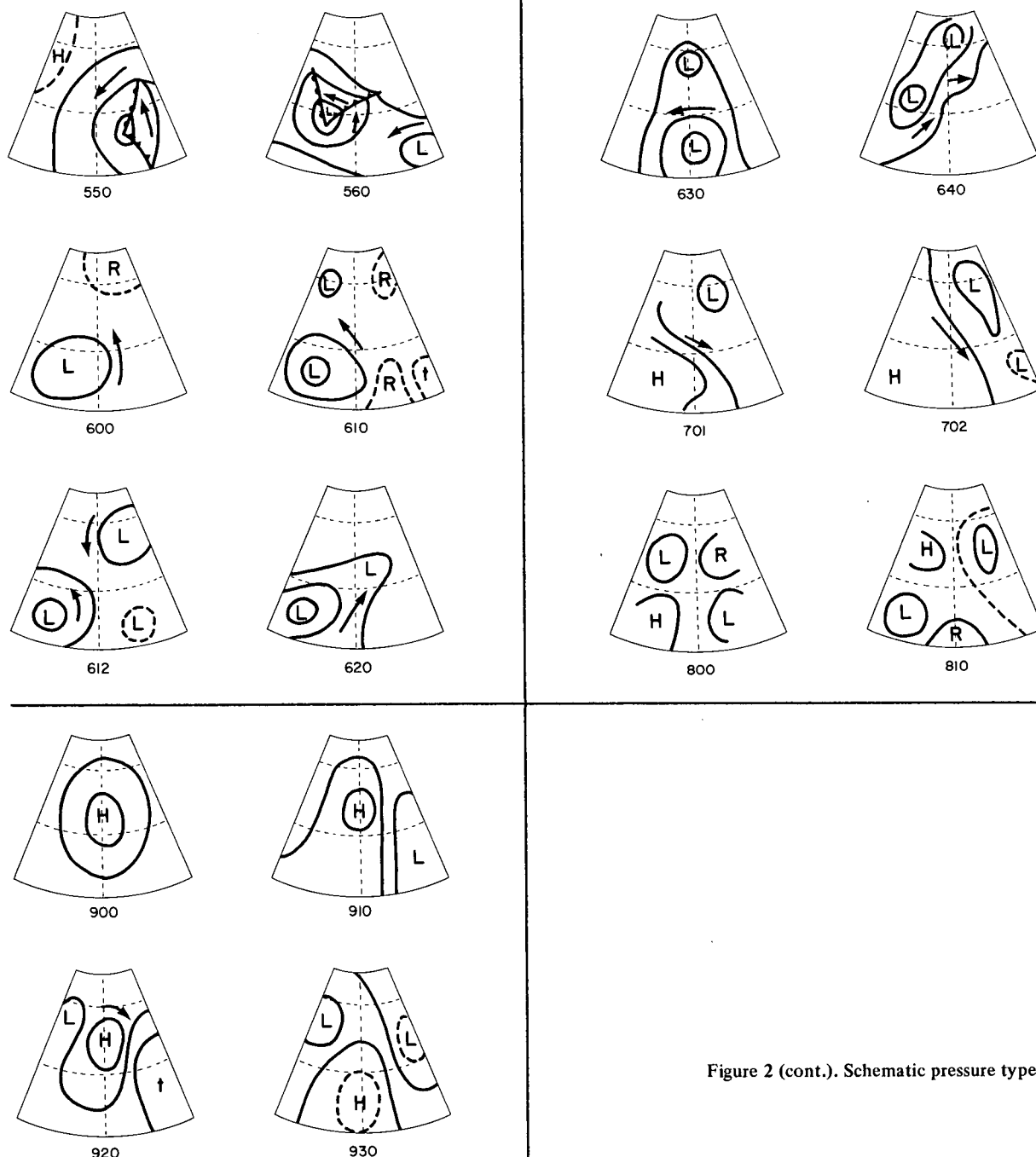


Figure 2 (cont.). Schematic pressure types.

2. the tens digit refers to an arbitrary numbering of types within these groups.

3. the units digit denotes a subtype, where 1 = anticyclonic subtype and 2 = cyclonic subtype.

The 500 mbar classification also uses a three digit coding:

1. the hundreds digit refers to the general flow direction over Baffin Island.

0 = Anticyclone	5 = S
1 = N	6 = SW
2 = NE	7 = W
3 = E	8 = NW
4 = SE	9 = Cyclone

0 and 9 are used when the circulation is dominated by a high (ridge) or low (trough), respectively.

2. the tens digit refers
 - (a) to curvature — anticyclonic = 0, cyclonic = 9 — if the hundreds digit is 1 to 8. Note that 00 — Anticyclone, 99 — Cyclone, 09 = Col (anticyclone or ridge dominated over Baffin), 90 = Col (low pressure dominant) or
 - (b) to the flow direction (1 to 8) if an anticyclonic or cyclonic system is setting up a fairly uniform flow.

3. the units digit indicates the sector (1-6) in which the main anticyclone or cyclone centre occurs (see Fig. 1). This is coded 0 if no centre occurs. Two special designations are:

(1-8), 0, 9 is the three figure code for a ridge over Baffin and major low centre elsewhere in the area,

(1-8), 9, 8 is the code for a trough over Baffin and a ridge or anticyclone elsewhere.

Table 1. Percentage Frequency of MSL Pressure-Pattern Types, 1961-65 and 1961-70 for July-August

Type	Jan-Feb (296 days)	April (150 days)	July-Aug (310 days) (620 days)		Sept-Oct (305 days)
100	4.4	3.2	6.1	5.6	7.5
101	0.7	0.7	1.6	0.8	1.6
102	4.7	0.7	2.6	3.2	1.3
110	1.7	1.3	3.6	2.9	1.6
120	5.7	4.0	2.9	2.4	4.9
130	0	0.7	5.2	3.5	2.6
200	0	0	0.3	0.3	0.3
210	1.4	1.3	1.0	0.6	0.7
220	4.1	4.0	4.8	3.5	11.1
300	0	0.7	2.6	2.1	0.3
310	1.0	4.0	1.9	3.5	2.0
320	0.7	3.2	3.6	4.7	0.7
400	0.3	0	0.3	0.5	0.3
410	1.0	0	2.6	4.5	0.7
420	1.4	2.0	2.3	2.4	1.6
430	0.7	2.7	2.9	2.4	4.3
500	1.7	2.7	7.1	5.2	5.6
510	3.4	1.3	2.6	2.6	5.6
511	5.1	2.7	2.3	1.8	2.9
520	6.3	4.0	0.6	0.3	2.9
521	5.7	8.0	2.3	1.9	1.6
531	5.1	14.0	5.8	3.5	2.3
532	2.0	0.7	0.3	0.6	2.0
540	1.7	0.7	0.6	0.8	1.3
542	5.1	0	1.6	1.6	2.6
550	1.0	0	0	0	0
560	0.7	0	0	0	0
600	2.4	4.7	7.4	6.1	3.6
610	1.7	1.3	3.2	4.0	2.6
612	1.7	0.7	1.3	1.8	2.3
620	1.0	0	1.9	1.8	2.6
630	1.0	1.3	4.2	5.0	3.3
640	1.4	0	0.3	0.6	1.0
701	5.1	9.3	1.6	1.6	0.7
702	7.1	2.0	1.6	1.9	6.2
800	2.0	0.7	3.2	3.9	0.7
810	2.4	0.7	1.6	2.1	1.0
900	2.4	4.7	2.3	3.9	1.6
910	0.7	1.3	1.9	1.9	1.0
920	2.4	10.7	1.4	2.7	3.6
930	0.7	0	0.6	1.5	1.3

TYPE FREQUENCY

The daily surface (MSL) and 500 mbar charts for 00 GMT (1900 EST of the previous day) have been classified into the categories set out above for July-August 1961-70, January-February, April and September-October 1961-65. Attention was concentrated on the summer period in view of its importance in terms of precipitation and for glaciological studies. Table 1 presents a summary of the results for the MSL pressure patterns.

In the winter months there is no single predominant type although the 500 group (low pressure in Labrador Sea-Baffin Bay sector) as a whole occurs on 39% of days and the 100 group (central low) on 17%. Similarly in the summer months these two groups account for 18% (23%, 1961-65) and 18% (22%, 1961-65) of the total, respectively, but again no single type predominates. In April, type 531 (anticyclone to west, trough in Davis Strait and low over Devon Island area) occurs on 14% of days, and type 920 (central anticyclone) on 11% of days, reflecting the mean pressure field at this season.

In September-October, type 220 (central ridge from the west, lows to north and south) is the most frequent (11%) individual type, the 500 group has a 27% frequency and the 100 group 19%.

Analysis of the precipitation and moisture flux characteristics of the types is discussed in the next chapter.

REFERENCES

- Barry, R. G. 1967. The prospect for synoptic climatology: a case study. In *Liverpool Essays in Geography* (Ed., Steel, R. W. and Lawton, R.), Longmans, 85-106.
- Blüthgen, J. 1965. Synoptische Klimageographie. *Geogr. Zeit.*, 53, 10-51.
- Hare, F. K. 1968. The Arctic. *Quart. J. R. Met. Soc.*, 94 (402): 439-59.
- Lund, I. A. 1963. Map-pattern classification by statistical methods. *J. Appl. Met.*, 2: 58-65.

3. The Synoptic Climatology of Precipitation and Moisture Flux

Contents

INTRODUCTION	Page 43
PRECIPITATION SYNOPTIC CLIMATOLOGY	43
VAPOUR-FLUX SYNOPTIC CLIMATOLOGY	45
CONCLUSIONS	46
REFERENCES	46

Illustrations

Figure 1. Isolines of horizontal vapour flux, $\text{g cm}^{-1}\text{s}^{-1}$, between the surface and a level in the upper troposphere where the flux is assumed to become zero (see Chapter 2). January – February 1961-65, type 100	49
Figure 2. Isolines of horizontal vapour flux, $\text{g cm}^{-1}\text{s}^{-1}$, between the surface and a level in the upper troposphere where the flux is assumed to become zero (see Chapter 2). January – February 1961-65, type 120	49
Figure 3. Isolines of horizontal vapour flux, $\text{g cm}^{-1}\text{s}^{-1}$, between the surface and a level in the upper troposphere where the flux is assumed to become zero (see Chapter 2). January – February 1961-65, type 510	49
Figure 4. Isolines of horizontal vapour flux, $\text{g cm}^{-1}\text{s}^{-1}$, between the surface and a level in the upper troposphere where the flux is assumed to become zero (see Chapter 2). January – February 1961-65, type 520	49
Figure 5. Isolines of horizontal vapour flux, $\text{g cm}^{-1}\text{s}^{-1}$, between the surface and a level in the upper troposphere where the flux is assumed to become zero (see Chapter 2). January – February 1961-65, type 550	50
Figure 6. Isolines of horizontal vapour flux, $\text{g cm}^{-1}\text{s}^{-1}$, between the surface and a level in the upper troposphere where the flux is assumed to become zero (see Chapter 2). July – August 1961-65, type 100	50
Figure 7. Isolines of horizontal vapour flux, $\text{g cm}^{-1}\text{s}^{-1}$, between the surface and a level in the upper troposphere where the flux is assumed to become zero (see Chapter 2). July – August 1961-65, type 110	50
Figure 8. Isolines of horizontal vapour flux, $\text{g cm}^{-1}\text{s}^{-1}$, between the surface and a level in the upper troposphere where the flux is assumed to become zero (see Chapter 2). July – August 1961-65, type 220	50
Figure 9. Isolines of horizontal vapour flux, $\text{g cm}^{-1}\text{s}^{-1}$, between the surface and a level in the upper troposphere where the flux is assumed to become zero (see Chapter 2). July – August 1961-65, type 300	51
Figure 10. Isolines of horizontal vapour flux, $\text{g cm}^{-1}\text{s}^{-1}$, between the surface and a level in the upper troposphere where the flux is assumed to become zero (see Chapter 2). July – August 1961-65, type 430	51
Figure 11. Isolines of horizontal vapour flux, $\text{g cm}^{-1}\text{s}^{-1}$, between the surface and a level in the upper troposphere where the flux is assumed to become zero (see Chapter 2). July – August 1961-65, type 500	51

Illustrations (cont.)

	Page
Figure 12. Isolines of horizontal vapour flux, $\text{g cm}^{-1}\text{s}^{-1}$, between the surface and a level in the upper troposphere where the flux is assumed to become zero (see Chapter 2). July – August 1961-65, type 600	51
Figure 13. Isolines of horizontal vapour flux, $\text{g cm}^{-1}\text{s}^{-1}$, between the surface and a level in the upper troposphere where the flux is assumed to become zero (see Chapter 2). July – August 1961-65, type 610	52
Figure 14. Isolines of horizontal vapour flux, $\text{g cm}^{-1}\text{s}^{-1}$, between the surface and a level in the upper troposphere where the flux is assumed to become zero (see Chapter 2). July – August 1961-65, type 620	52
Figure 15. Isolines of horizontal vapour flux, $\text{g cm}^{-1}\text{s}^{-1}$, between the surface and a level in the upper troposphere where the flux is assumed to become zero (see Chapter 2). September – October 1961-65, type 100	52
Figure 16. Isolines of horizontal vapour flux, $\text{g cm}^{-1}\text{s}^{-1}$, between the surface and a level in the upper troposphere where the flux is assumed to become zero (see Chapter 2). September – October 1961-65, type 120	52
Figure 17. Isolines of horizontal vapour flux, $\text{g cm}^{-1}\text{s}^{-1}$, between the surface and a level in the upper troposphere where the flux is assumed to become zero (see Chapter 2). September – October 1961-65, type 220	53
Figure 18. Isolines of horizontal vapour flux, $\text{g cm}^{-1}\text{s}^{-1}$, between the surface and a level in the upper troposphere where the flux is assumed to become zero (see Chapter 2). September – October 1961-65, type 500	53
Figure 19. Isolines of horizontal vapour flux, $\text{g cm}^{-1}\text{s}^{-1}$, between the surface and a level in the upper troposphere where the flux is assumed to become zero (see Chapter 2). September – October 1961-65, type 510	53
Figure 20. Isolines of horizontal vapour flux, $\text{g cm}^{-1}\text{s}^{-1}$, between the surface and a level in the upper troposphere where the flux is assumed to become zero (see Chapter 2). September – October 1961-65, type 630	53
Figure 21. Isolines of horizontal vapour flux, $\text{g cm}^{-1}\text{s}^{-1}$, between the surface and a level in the upper troposphere where the flux is assumed to become zero (see Chapter 2). September – October 1961-65, type 702	54

Tables

1. Precipitation in relation to pressure pattern types in January-February, 1961-65	43
2. Precipitation in relation to pressure pattern types in July-August, 1961-65	44
3. Precipitation in relation to pressure pattern types in September-October, 1961-65	44
4. Precipitation in relation to pressure pattern types in July-August, 1961-70	45

The Synoptic Climatology of Precipitation and Moisture Flux

INTRODUCTION

The catalogue of daily MSL pressure fields for the area 55° - 80° N, 50° - 100° W has been applied to a consideration of precipitation and moisture flux characteristics over Baffin Island. The computation of horizontal vapour flux with respect to each type of pressure pattern was determined for January and February, July and August, and September and October 1961-65 using a modified version of programme C70103 (Canadian Department of Energy, Mines and Resources) developed by K. Shimizu in co-operation with the author. Computations were carried out on the CDC 3200 system by K. Shimizu, by arrangement with Dr. J. G. Fyles, Geological Survey of Canada.

As a basis for considering the fluxes associated with more important precipitation-producing patterns, first examined will be the contribution of each pattern to the January-February, July-August, and September-October precipitation at Broughton Island and Cape Dyer on the east coast and at Dewar Lakes, inland. The proportion of mean annual precipitation (1960-64) in these pairs of months at the selected station is:

	January-February	July-August	September-October	Mean Annual Total
Broughton Island	8.3%	13.0%	36.9%	11.74 in.
Cape Dyer	17.7	15.5	23.9	26.40
Dewar Lakes	4.4	42.8	26.8	8.55

PRECIPITATION SYNOPTIC CLIMATOLOGY

Tables 1-3 show the types accounting for at least 5% of the bimonthly precipitation over the five years. It should be noted that the type catalogue refers to the 00 GMT map so that the precipitation for the preceding day (06-06 GMT) has been used. Dewar Lakes has been excluded from Table 1 in view of the very low precipitation in mid-winter.

In all three seasons a rather few types contribute the major proportion of the precipitation and on a smaller percentage of all days with measurable precipitation. However, the precipitation-producing types differ seasonally and also spatially. In view of the close proximity of Broughton Island and Cape Dyer the present results bear out the earlier findings of Andrews, Barry and Drapier

(1970) concerning extreme local variability of precipitation with synoptic-scale patterns.

In January-February, types 100 and 102 are significant at both east coast stations. Also, in spite of the percentage contrast, type 550 gives similar absolute totals at the two stations. The importance of this type in view of its infrequent occurrence is of particular interest.

Types 100, 500, and 610 in summer and 100 and 510 in autumn produce significant precipitation at all three stations. Types with a low to west or southwest (430 in summer and 620, 630 in autumn) are mainly important at Dewar Lakes and types with low pressure in Davis Strait-Baffin Bay are important in southeastern Baffin Island. There is no immediately apparent reason for the discrepancies between Broughton Island and Cape Dyer for types 220, 300, and 600 in summer, or types 310, 531, and 542 in autumn.

Table 1. Precipitation in Relation to Pressure Pattern Types in January-February, 1961-65 (percent of total)

Type	Description	Broughton Is.	Cape Dyer
100	Low centered over Baffin, high to S	7.3	17.8
102	Low centered over Baffin, no high to S	9.5	16.7
120	Lows in Foxe Basin, N. Hudson Bay and Davis Strait, ridge over Hudson Strait	7.6	
510	E-NE flow, low in N. Labrador Sea area with low or trough also in Baffin Bay	8.4	
520	N flow, trough Davis Strait, high to W		8.4
550	Low Davis Strait, warm front N-S in Baffin Bay	37.7	11.2
620	Low in Hudson Bay and trough to Baffin Bay	10.9	
910	High Baffin, trough Baffin Bay	5.5	
Total precipitation, Jan.-Feb. 1961-65		5.49 in	29.85 in
Percentage of total with above types		86.7	54.1
Percentage of precipitation days giving above proportion		49	31

Table 2. Precipitation in Relation to Pressure Pattern Types in July-August, 1961-65 (percent of total)

Type	Description	Broughton Is.	Cape Dyer	Dewar Lakes
100	Low centred over Baffin, high to S	18.6	17.6	21.6
102	Low centred over Baffin, no high to S			5.8
110	Trough over Baffin and high to S	10.8		12.6
130	Low over Baffin and lows or troughs to SE and SW	14.8		10.9
220	Lows in northern Baffin Bay and Hudson Bay. Ridge from W over Baffin Island		7.7	
300	Low Hudson Strait, High over Baffin; E flow		7.2	
430	Lows to SW and W, ridge to SE			7.3
500	E flow, low in N. Labrador Sea area	7.5	7.3	7.2
600	S flow, low N. Hudson Bay		18.1	
610	S-SE flow, low N. Hudson Bay and trough to N, ridge in Baffin Bay	7.7	6.4	5.8
620	Low in Hudson Bay and trough to Baffin Bay	6.2	7.0	
702	Low over northern Baffin Bay	5.5		
810	Ridges to W and S, lows Hudson Bay and Baffin Bay	5.5		
Total precipitation, July-August 1961-65		6.00 in	17.58 in	19.01 in
Percentage of total with above types		68.9	64.9	65.4
Percentage of precipitation days giving above proportion		37	50	43

Table 3. Precipitation in Relation to Pressure Pattern Types in September-October, 1961-65 (percent of total)

Type	Description	Broughton Is.	Cape Dyer	Dewar Lakes
100	Low centred over Baffin, high to S	6.2	16.2	17.0
120	Lows in Foxe Basin, N. Hudson Bay and Davis Strait, ridge over Hudson Strait	7.3		
130	Low over Baffin and lows or troughs to SE and SW			6.4
220	Lows in northern Baffin Bay and Hudson Bay. Ridge from W over Baffin Island	11.4		
310	E flow, ridge to N, lows to SW and SE	5.9		
500	E flow, low in N. Labrador Sea area	5.9	11.5	
510	E-NE flow, as 500 with low or trough also in Baffin Bay	5.5	14.2	9.5
531	Ridge over S. Baffin, low N. Baffin and trough Davis Strait	6.8		
542	Low in N. Labrador Sea, trough/ low Foxe Basin		5.1	
612	Lows N. Hudson Bay, Baffin Bay, N. Labrador Sea	5.5		
620	Low in N. Hudson Bay and trough to Baffin Bay			8.8
630	Low Hudson Strait and N. Baffin Island			8.3
702	NW flow, low N. Baffin Bay	11.6	10.2	14.5
Total precipitation, Sept.-Oct. 1961-65		21.83 in	29.38 in	10.56 in
Percentage of total with above types		66.1	66.4	64.5
Percentage of precipitation days giving above proportion		57	66	49

Table 4. Precipitation in Relation to Pressure Pattern Types in July-August, 1961-70 (percent of total)

Type	Description	Broughton Is.	Cape Dyer	Dewar Lakes
100	Low centred over Baffin, high to S	13.2	15.8	19.0
102	Low centred over Baffin, no high to S	6.9	10.4	12.6
110	Trough over Baffin and high to S	8.9		8.5
130	Low over Baffin and lows or troughs to SE and SW	7.8		6.4
300	Low Hudson Strait, High over Baffin; E flow		5.2	
310	E flow, ridge to north, lows to SW, SE		6.1	
500	E flow, low in N. Labrador Sea area	6.7	7.2	5.1
510	E-NE flow, as 500 with low or trough also in Baffin Bay	7.8	7.4	
600	S flow, low N. Hudson Bay	7.1	11.1	
Total precipitation, July-August 1961-70		12.17 in	33.63 in	36.75 in
Percentage of total with above types		58.4	63.2	51.6
Percentage of precipitation days giving above proportion		41	44	35

As an extension of this analysis, in view of the significance of summer precipitation from the standpoint of glaciological mass-balance studies, the precipitation characteristics of the pressure patterns have been evaluated for the period July-August, 1961-70. Table 4, when compared with Table 2, shows that types 100 (and 102), 110, 130, 300, 500, and 600 feature significantly in both periods. In view of the variability of falls, affecting the calculated percentages, this provides greater confidence in the generality of the results. At the same time there is evidently a rather great spread of types contributing 40-50% of the total precipitation.

VAPOUR-FLUX SYNOPTIC CLIMATOLOGY

The analysis of patterns of total and eddy horizontal flux of water vapour follows similar lines to previous studies for Labrador-Ungava (Barry, 1967). However, the synoptic types defined for Baffin Island are more suitable for this purpose since the static pressure field is classified instead of regionally-variable flow patterns. Most of the patterns which are sources for one or other of the three stations examined in section 2 are discussed here.

Figures 1-5 show the flux patterns for types contributing much of the mid-winter precipitation in east Baffin Island. These maps give some impression of flux convergence in the simpler cases. Convergence will be large when the flux vector is perpendicular to the isolines and directed towards lower values. Type 100 has large northward flux in this area and, for winter, high precipitable water content over Baffin Bay. Average January values are 1.5-3 mm (Barry and Fogarasi, 1968). Type 102, not shown, has a very similar distribution. Type 120 (Figure 2) has a rather weak pattern. With type 510 (Figure 3) the flux is easterly and the moisture content is about average,

whereas with type 520 flux is much weaker from the southeast (Figure 4). There is no apparent reason why precipitation occurs mainly at Broughton Island with the former, and at Cape Dyer with the latter pattern. The infrequent, but distinctive 550 type (Figure 5) has very high precipitable water content for winter and strong southeasterly flux.

The pattern of flux with 100 type, which is an important precipitation source at all three stations in July, (Figure 6) is quite different from that in winter; there is now a large latitudinal decrease as well as evidence of cyclonic circulation. Again, type 102 is broadly similar to 100. Figure 7 shows westerly flux decreasing eastward with type 110. Type 130, not shown, is very similar to Figure 6 for type 100 but with a slightly weaker pattern. There is no evident reason for types 110 and 130 to make significant contributions to the precipitation at Broughton Island and Dewar Lakes but not at Cape Dyer. Conversely, the next two types, 220 (Figure 8) with northwesterly to northerly flux and 300 (Figure 9) with strong easterly flux are both important at Cape Dyer, but not at the other two stations. The significance of type 430 (Figure 10) at Dewar Lakes is apparently related to the strong southwesterly flux. Type 500 (Figure 11) which is important at all three stations has strong easterly flux. Here the total flux vector is towards higher values and it is probably the eddy component which is important. Type 600 (Figure 12) shows strong southerly flux and high moisture contents compared with an average of about 14-15 mm over Frobisher. This pattern is very significant at Cape Dyer (18% of the July-August total precipitation for 1961-65), but not at the other two stations. Type 610 which is important at all three stations shows a rather weaker southerly flux (Figure 13). Finally, type 620 (Figure 14), which is important at Dewar Lakes and Broughton Island, is associated with southwesterly flux and average or above moisture content.

The September-October pattern of type 100 (Figure 15) is comparable with that of summer though with larger flux values. The precipitable water content is large, compared with an average of 7-8 mm over Frobisher at this season. Type 120 (Figure 16) showing strong southwesterly flux is, strangely, important at Broughton Island but not at Dewar Lakes. Type 130, not shown, which is important at Dewar Lakes has a similar flux pattern to 100 but less moisture is available. Type 220 (Figure 17), which is only important at Broughton Island, shows northwesterly flux. Type 500 (Figure 18) which is associated with easterly flux is clearly important along the east coast of Baffin Island. Type 510 (Figure 19) which has north-northeasterly flux is also important in the same area, though it is less obvious why this pattern should contribute significantly to the precipitation at Dewar Lakes. Types 620, not shown, and 630 (Figure 20), which are both important at Dewar Lakes, have very similar patterns. The flux values are somewhat larger with 630 although the moisture contents are lower but still above the seasonal average. The last type 702 (Figure 21) is important at all three stations. This would not be expected at the east coast stations since the flux is from the northwest.

CONCLUSIONS

The application of the synoptic classification to a consideration of precipitation and moisture flux has provided useful information. Thus, approximately 65% of the precipitation in summer and autumn can be attributed to some 6-8 MSL pressure pattern types. In winter the proportion is even higher at Broughton Island.

The patterns of horizontal vapour flux have been determined for each pressure pattern type in January-February, July-August, and September-October, 1961-65. While some relationships between vapour flux and precip-

itation characteristics are readily apparent, it is evident that computation of the flux-divergence patterns is required as a basis for further explanation of precipitation occurrence. It is hoped to pursue this problem at a later date. Even so, it must be recognized that satisfactory results may not be obtainable in view of local variability compared with the synoptic scale of analysis and the known sampling problems on shorter time scales (Rasmusson, 1971) as discussed in the previous section. At least the foundation of a better understanding of the precipitation climatology of Baffin Island has now been laid.

Note added in proof: The change in frequency of groups of the types in July-August between 1961-65 and 1966-70 has been recently examined with respect to changes in climate and evidence for increased glacierization in Baffin Island (Bradley and Miller, 1972).

REFERENCES

- Andrews, J. T., Barry, R. G. and Drapier, L. 1970. An inventory of the present and past glacierization of Home Bay and Okoa Bay, east Baffin Island, N.W.T., Canada, and some climatic and palaeoclimatic considerations. *J. Glaciol.* 9, (57): 337-362.
- Barry, R. G. 1967. Variations in the content and flux of water vapour over eastern North America during two winter seasons. *Quart. J. R. Met. Soc.* 93: 535-543.
- Barry, R. G. and Fogarasi, S. 1968. Climatological studies of Baffin Island, N.W.T. *Tech. Bull. No. 13*, Inland Waters Branch, Department of Energy, Mines and Resources, Ottawa, 106pp.
- Bradley, R. S. and Miller, G. H. 1972. Recent climatic changes and increased glacierization in the eastern Canadian Arctic. *Nature* 237: 385-387.
- Rasmusson, E. M. 1971. A study of the hydrology of eastern North America using atmospheric flux data. *Mon. Wea. Rev.* 99: 119-135.

Figures 1-21

Isolines of horizontal vapour flux, $\text{g cm}^{-1}\text{s}^{-1}$,
between the surface and a level in the upper troposphere
where the flux is assumed to become zero.

Plotting Model

Solid arrow: total flux

dashed arrow: eddy flux

number above station: total vapour content (mm
precipitable water)

upper number to right: total flux

lower number to right: eddy flux

number to left (parentheses): number of observations
for the type

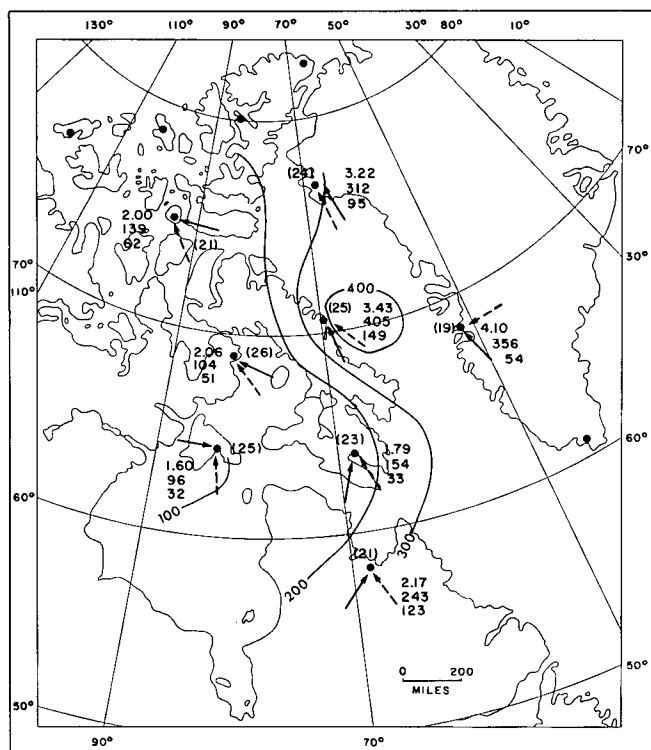


Figure 1. January–February 1961-65, type 100.

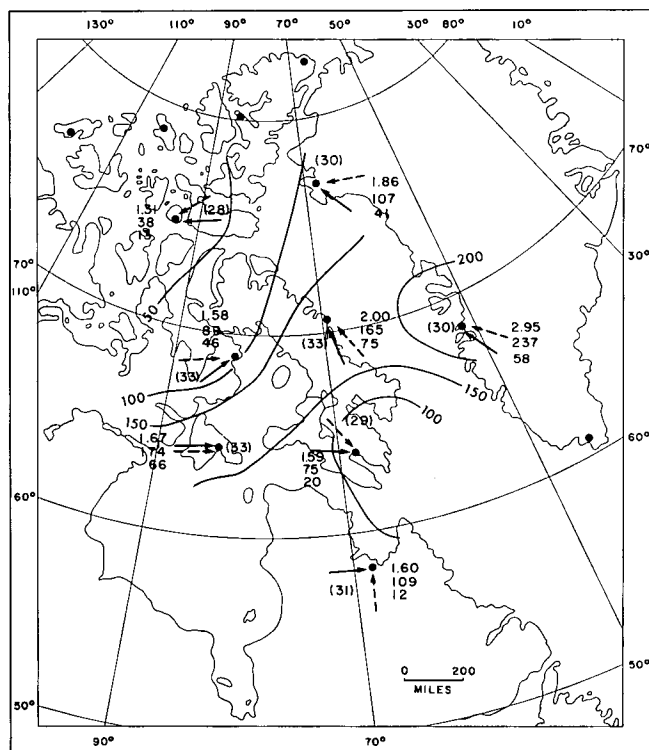


Figure 2. January–February 1961–65, type 120.

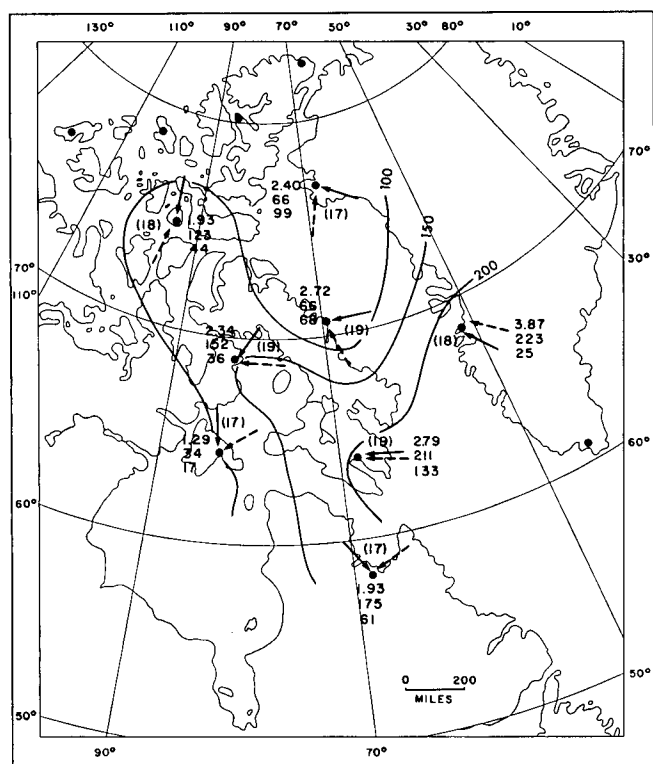


Figure 3. January–February 1961-65, type 510.

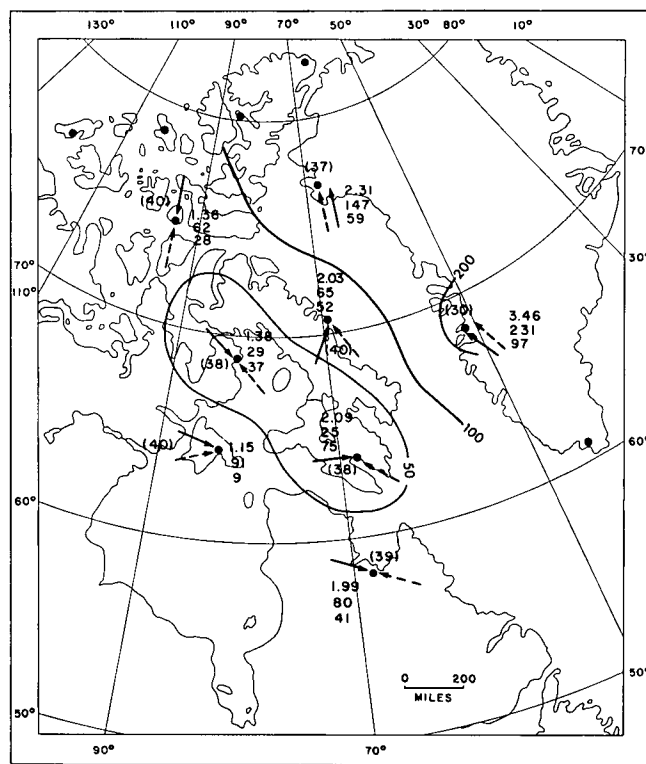


Figure 4. January–February 1961-65, type 520.

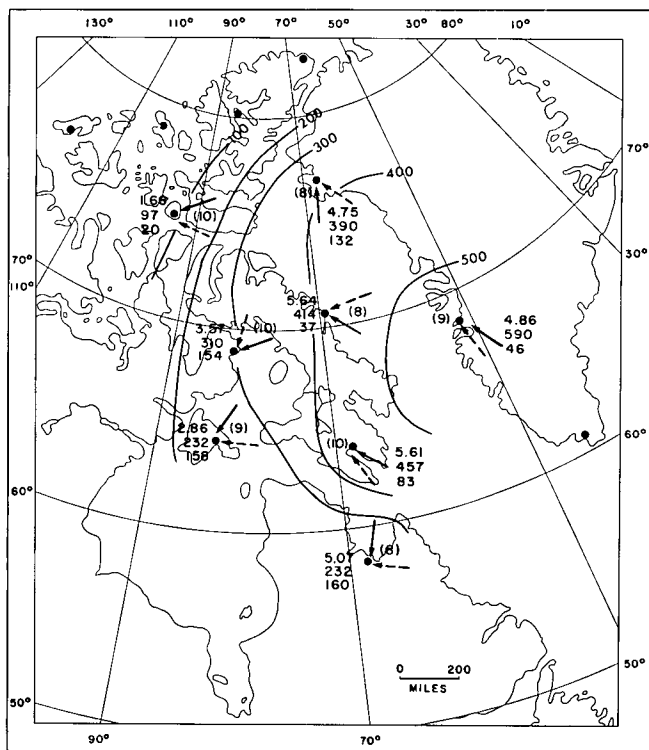


Figure 5. January-February 1961-65, type 550.

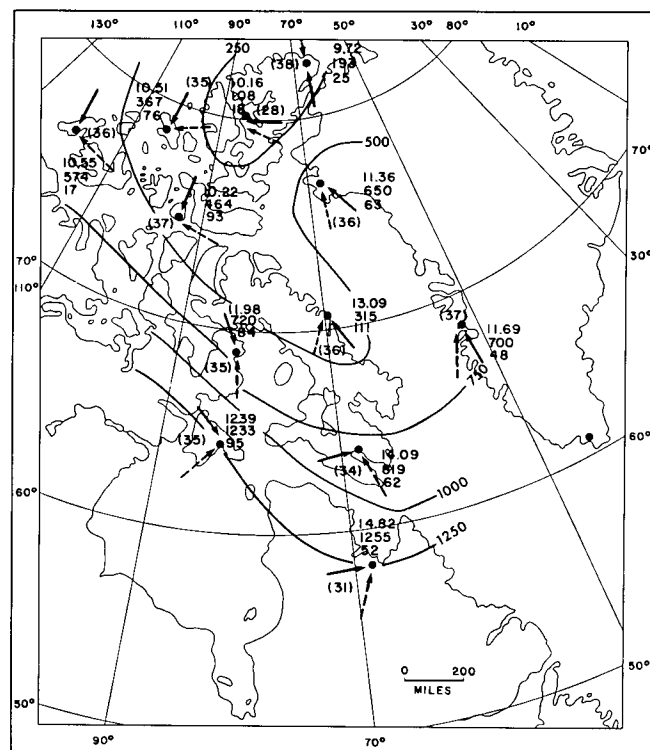


Figure 6. July-August 1961-65, type 100.

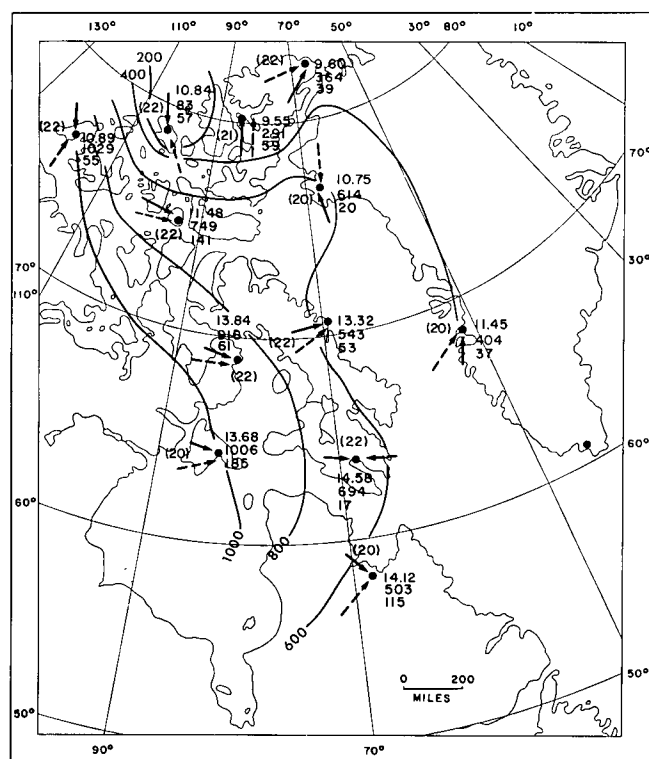


Figure 7. July-August 1961-65, type 110.

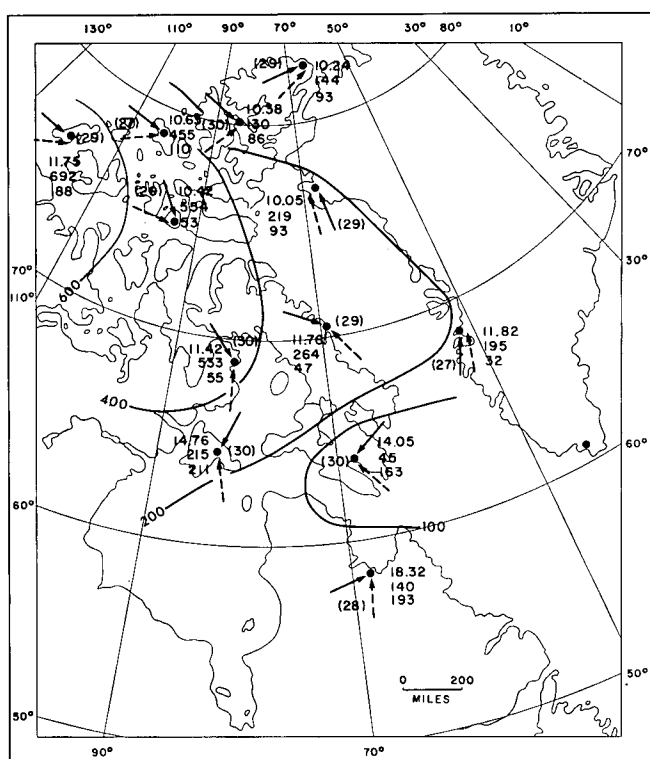


Figure 8. July-August 1961-65, type 220.

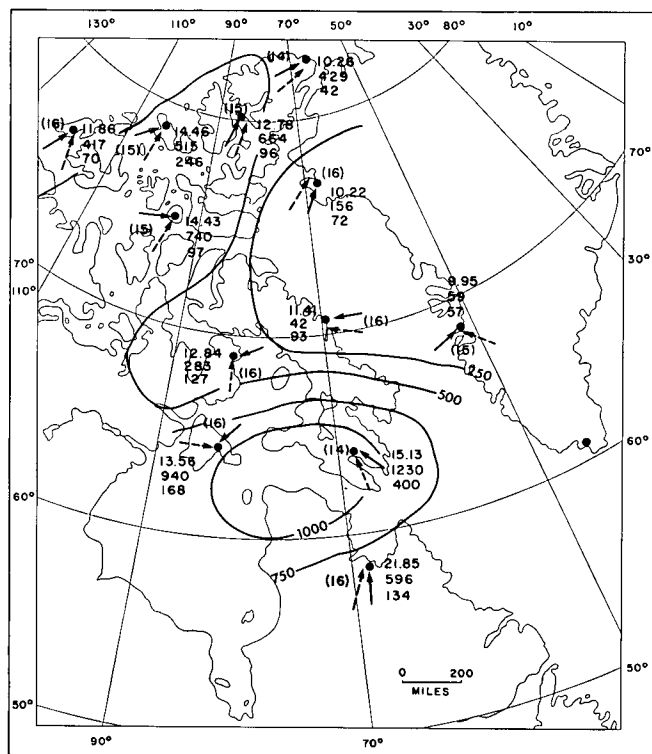


Figure 9. July-August 1961-65, type 300.

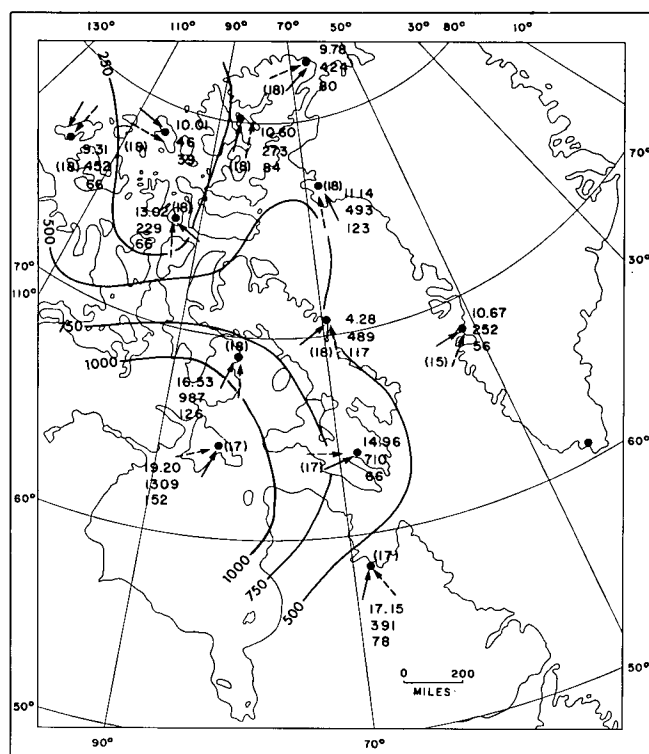


Figure 10. July-August 1961-65, type 430.

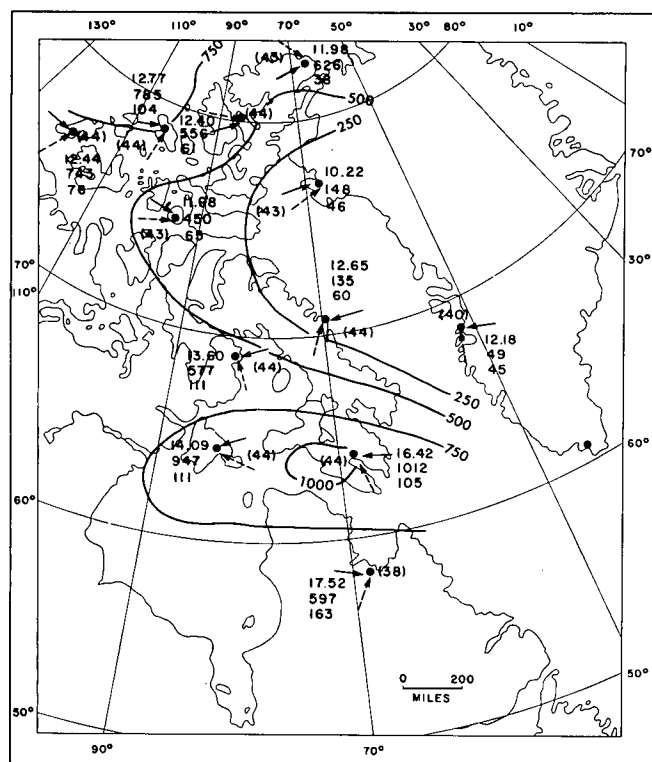


Figure 11. July-August 1961-65, type 500.

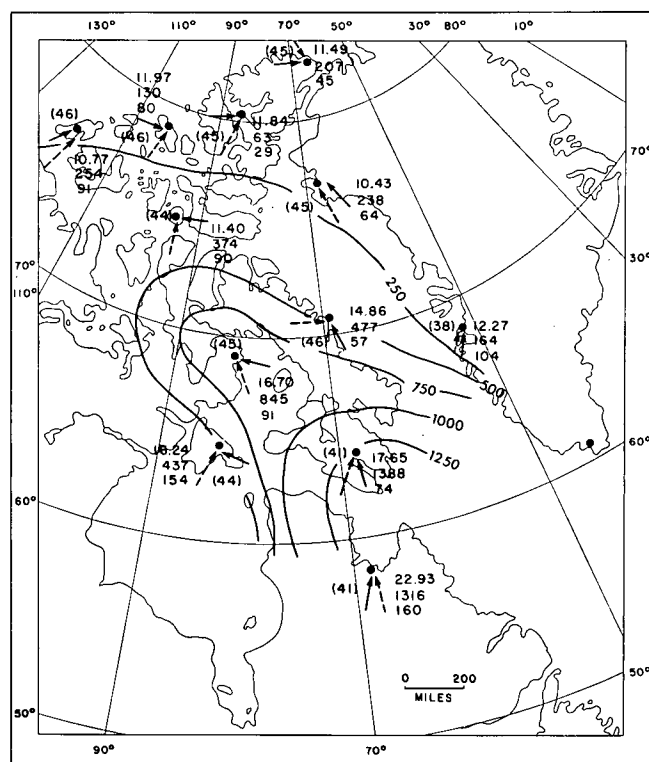


Figure 12. July-August 1961-65, type 600.

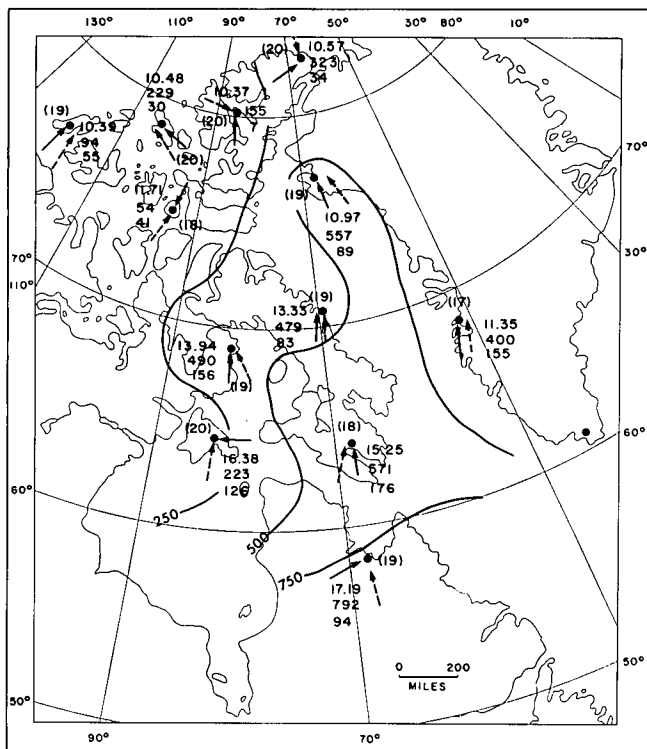


Figure 13. July-August 1961-65, type 610.

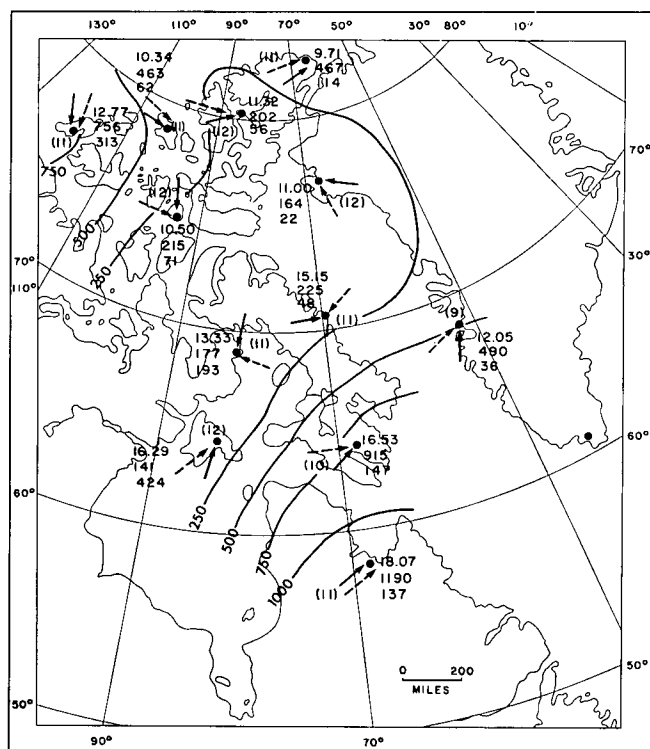


Figure 14. July-August 1961-65, type 620.

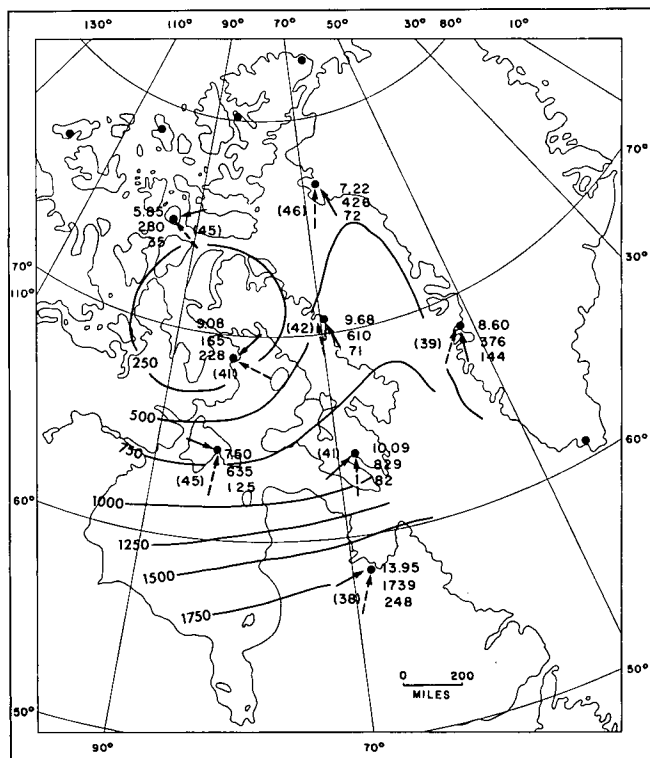


Figure 15. September-October 1961-65, type 100.

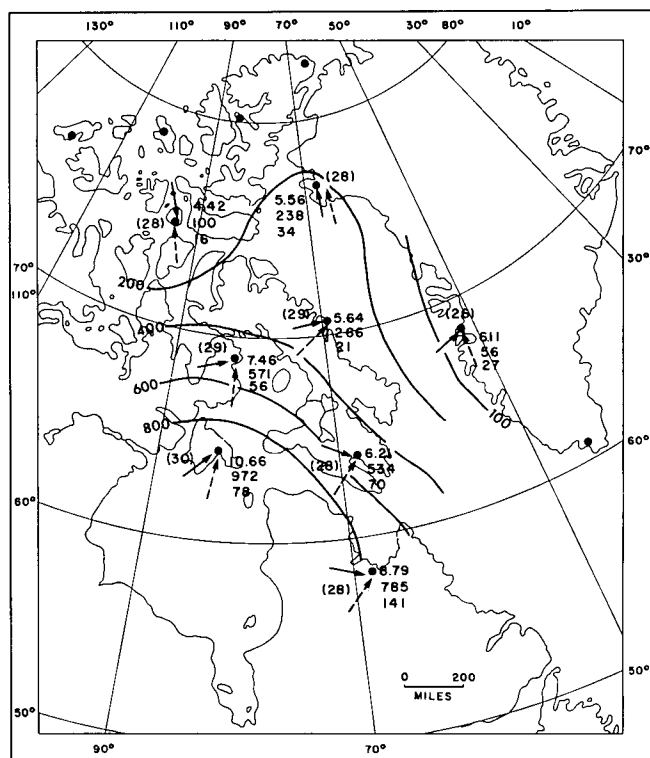


Figure 16. September-October 1961-65, type 120.

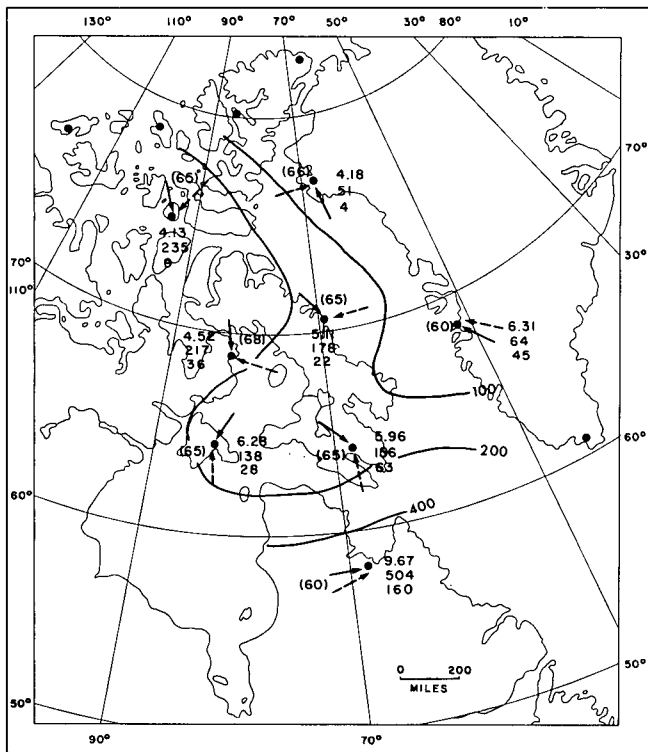


Figure 17. September-October 1961-65, type 220.

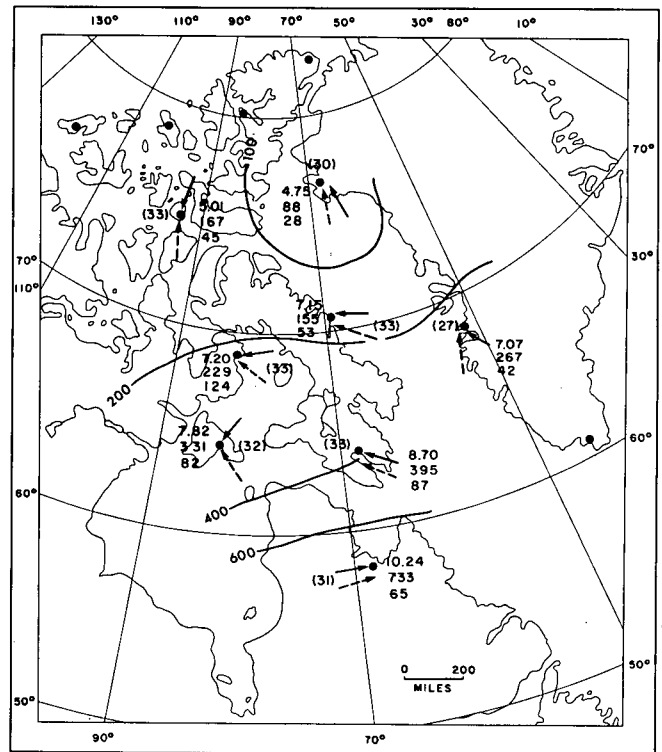


Figure 18. September-October 1961-65, type 500.

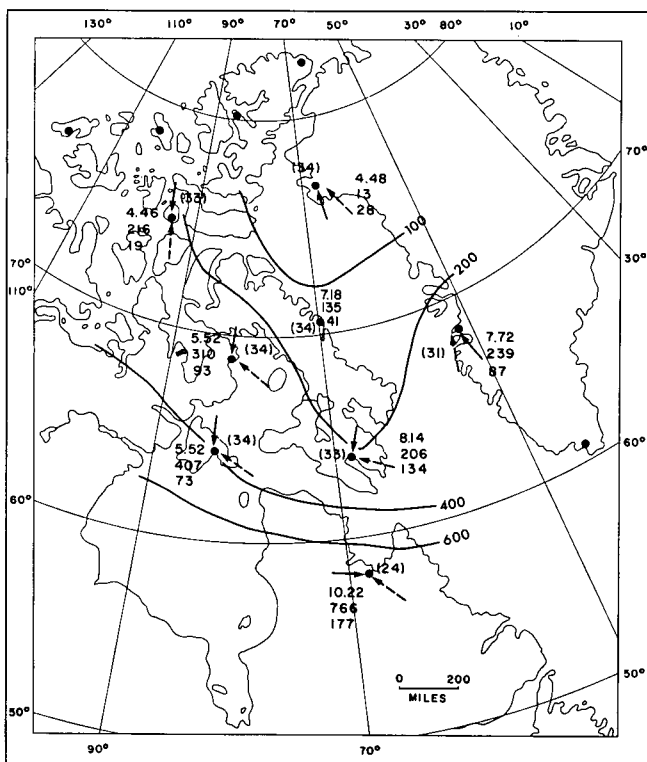


Figure 19. September-October 1961-65, type 510.

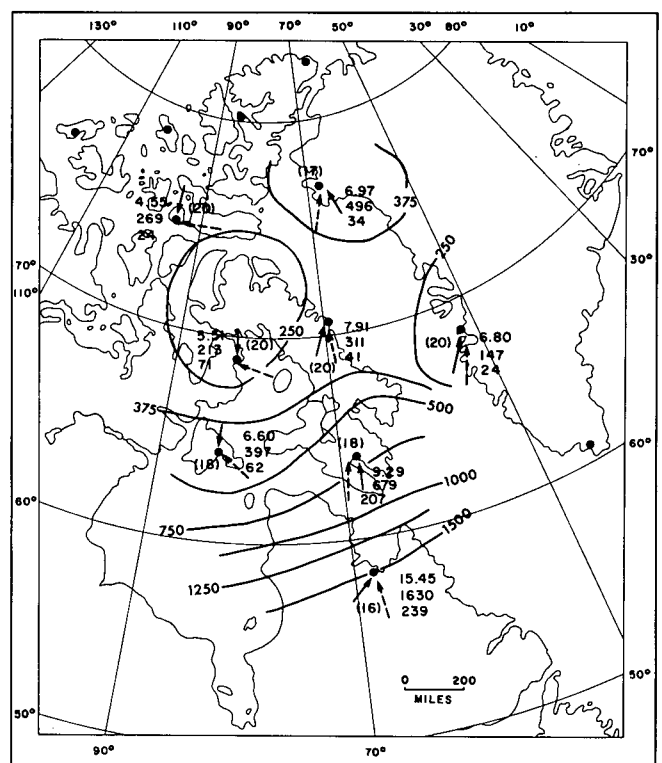


Figure 20. September-October 1961-65, type 630.

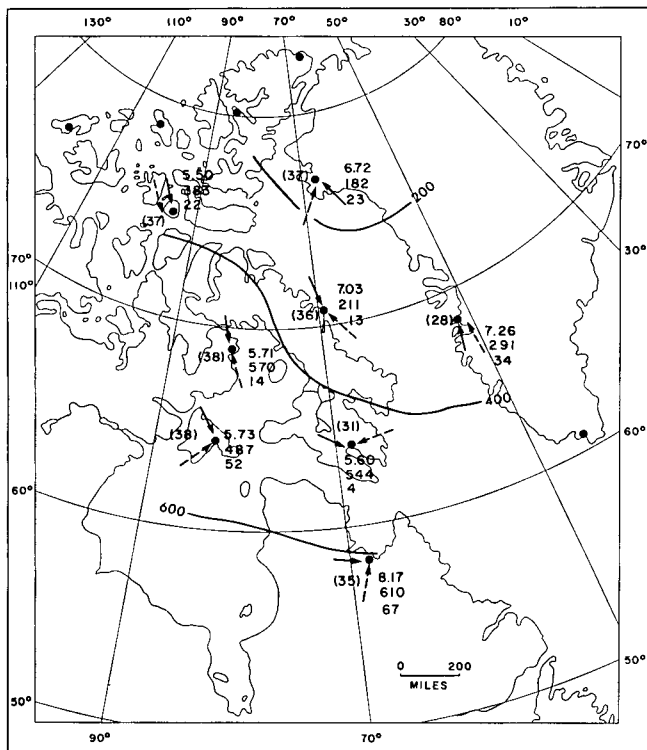


Figure 21. September-October 1961-65, type 702.